Spectral functions and rf response of ultracold fermionic atoms

R. Haussmann,[1] M. Punk,[2] and W. Zwerger[2]

[1]*Fachbereich Physik, Universität Konstanz, D-78457 Konstanz, Germany*
[2]*Physikdepartment, Technische Universität München, D-85748 Garching, Germany*

We present a calculation of the spectral functions and the associated rf response of ultracold fermionic atoms near a Feshbach resonance. The single-particle spectra are peaked at energies that can be modeled by a modified BCS dispersion. However, even at very low temperatures their width is comparable to their energy except for a small region around the dispersion minimum. The structure of the excitation spectrum of the unitary gas at infinite scattering length agrees with recent momentum-resolved rf spectra near the critical temperature. A detailed comparison is made with momentum integrated, locally resolved rf spectra of the unitary gas at arbitrary temperatures and shows very good agreement between theory and experiment. The pair size defined from the width of these spectra is found to coincide with that obtained from the leading gradient corrections to the effective-field theory of the superfluid.

I. INTRODUCTION

The existence of well-defined noninteracting quasiparticles above a possibly strongly correlated ground state is a central paradigm of many-body physics. In interacting Fermi systems, this concept applies both in a Fermi liquid and in a BCS-like superfluid state, whose elementary excitations have an infinite lifetime at the Fermi surface. More generally, the nature of quasiparticle excitations may be used to characterize many-body ground states both with and without long-range order [1]. Typically, it is only near a quantum phase transition between ground states with different types of order where a quasiparticle description fails and is replaced by a continuum of gapless excitations [2]. In our present work, we discuss ultracold fermionic atoms with a tunable attractive interaction. The ground state is a neutral *s*-wave superfluid at arbitrary coupling. Thus, it has gapless bosonic quasiparticles of the Bogoliubov-Anderson type with a linear spectrum $\omega = c_s q$. Its fermionic excitations have a finite gap. Within a BCS description, the associated Bogoliubov quasiparticles are exact eigenstates of the interacting system at arbitrary momenta. As will be shown below, this central feature of the BCS picture of fermionic superfluids fails for the strong coupling situation that is relevant in the cold gases context, where the excitation energy is no longer exponentially small compared with the Fermi energy. In this regime, the fermionic particle excitations acquire a significant lifetime broadening even at zero temperature, except near the dispersion minimum (or maximum for holes), where there is no available phase space for decay. The lifetime broadening arises both from the residual interaction between quasiparticles and their coupling to the collective sound mode. Moreover, the particle-hole symmetry characteristic for the Bogoliubov quasiparticles of the BCS theory is violated in the strong coupling regime. With increasing temperatures, the particle-like and holelike branches merge into a single broad excitation branch with a free-particle-like dispersion shifted by the binding energy.

Fermions with a tunable attractive interaction and the associated BCS-BEC crossover have been studied experimentally using ultracold Fermi gases near a Feshbach resonance [3–5]. The fact that the balanced system with an equal number of particles in the two different hyperfine states ("spins") that undergo pairing is superfluid at sufficiently low temperatures has been inferred from the observation of a finite condensate fraction on the BCS side [6] and from the collective mode frequencies in a trap that agree with superfluid hydrodynamics [7,8]. It was demonstrated quite directly by the observation of a vortex lattice in the rotating gas, which evolves continuously from the Bose-Einstein condensate (BEC) to the BCS side of the transition [9]. To study the excitation spectrum, in particular the evolution of the expected gap for fermionic excitations due to pairing, rf spectroscopy was performed by Chin *et al.* [10]. The interpretation of these measurements [11] in terms of an effective "pairing gap," however, is made difficult by the existence of strong final state interactions and the fact that the signal is an average over the whole cloud, with a spatially dependent excitation gap. For a homogeneous system, the average rf shift is in fact dominated by large mean-field effects and final state interactions [12–15] and is hardly changed, even if superfluidity is suppressed by a rather strong imbalance [16]. The problems associated with final state interactions and the inhomogeneity of the cloud have been overcome only recently by the possibility to perform spatially resolved rf measurements [17], combined with a suitable choice of the hyperfine states which undergo pairing and the final state of the rf transition [18]. Moreover, it has also become possible to measure rf spectra in a momentum-resolved way [19]. This opens the possibility to infer the full spectral functions as suggested theoretically by Dao *et al.* [20].

Our aim in the following is to present a calculation of the spectral functions and the associated rf response of strongly interacting fermions which covers the whole regime of temperatures both above and below the superfluid transition and also arbitrary coupling constants. The theory is based on a conserving, so-called Φ-derivable approach to the many-body problem due to Luttinger and Ward, in which the exact one-particle Green's functions serve as an infinite set of variational parameters. This approach has been used previously to describe the thermodynamic properties of the uni-

form [21] and the trapped gas [22]. The Luttinger-Ward formulation of the many-body problem relies on expressing the thermodynamic potential $\Omega[G]$ in terms of the exact Green's function G. The condition that the functional $\Omega[G]$ is stationary with respect to small variations in the Green's functions then leads to a set of integral equations for the matrix Green's function G which have to be solved in a self-consistent manner. Since the Green's functions contain information about the full dynamical behavior via the imaginary time dependence of the Matsubara formalism, the Luttinger-Ward approach not only provides results for the equilibrium thermodynamic quantities but also determines the full spectral functions upon analytic continuation from Matsubara to real frequencies. This is done explicitly in our present work using the maximum-entropy technique.

The paper is organized as follows: in Sec. II we introduce the Luttinger-Ward formalism and discuss the calculation of the momentum and frequency-dependent spectral functions. The relation between the spectral functions and the experimentally measured rf spectra is outlined in general and discussed in the BCS and BEC limit, where analytical results are available. We also discuss the behavior of the rf spectra at high frequencies and the associated contact coefficient introduced by Tan [23] and by Braaten and Platter [24]. In Sec. III, we show that a pair size can be defined via the momentum dependence of the superfluid response in analogy to the nonlocal penetration depth in superconductors. Using an effective-field theory due to Son and Wingate [25], we find that the resulting pair size of the unitary gas coincides with that inferred experimentally from the width of the rf spectrum [18]. The numerical results and the physical interpretation of spectral functions and rf spectra obtained within the Luttinger-Ward approach are discussed in Sec. IV, both in the normal and superfluid phase. These results are compared quantitatively with measured data. A summary and discussion are given in Sec. V. There are two appendixes, one on the maximum-entropy method and one on a perturbative calculation of the quasiparticle lifetime due to interactions with the collective mode.

II. LUTTINGER-WARD THEORY, SPECTRAL FUNCTIONS, AND RF RESPONSE

Our calculation of the spectral functions for a dilute system of ultracold fermionic atoms is based on a Luttinger-Ward approach to the BCS-BEC crossover that has been presented in detail previously [21,26]. As a starting point, we use the standard single-channel Hamiltonian that contains the essential physics of the BCS-BEC crossover in a dilute gas of ultracold fermionic atoms with a short-range (s-wave) interaction [4]

$$\hat{H} = \int d^3r \sum_\sigma \frac{\hbar^2}{2m} [\nabla \psi_\sigma^+(\mathbf{r})][\nabla \psi_\sigma(\mathbf{r})]$$

$$+ \frac{g_0}{2} \int d^3r \sum_\sigma \psi_\sigma^+(\mathbf{r}) \psi_{-\sigma}^+(\mathbf{r}) \psi_{-\sigma}(\mathbf{r}) \psi_\sigma(\mathbf{r}). \quad (2.1)$$

Here $\psi_\sigma(\mathbf{r})$ and $\psi_\sigma^+(\mathbf{r})$ are the usual fermion field operators. The formal spin index σ labels two different hyperfine states

which interact via a zero-range delta potential $g_0 \delta(\mathbf{r})$. Since a delta function in three dimensions leads to no scattering at all, the bare coupling strength

$$g_0(\Lambda) = \frac{g}{1 - 2a\Lambda/\pi} \quad (2.2)$$

needs to be expressed in terms of renormalized scattering amplitude $g = 4\pi\hbar^2 a/m$ that is proportional to the s-wave scattering length a and an ultraviolet momentum cutoff Λ that is taken to infinity at fixed g. The limiting process $g_0(\Lambda \to \infty) \to -0$ accounts for the replacement of the bare delta potential by a pseudopotential with the proper scattering length. The description of a Feshbach resonance by a single-channel Hamiltonian of the form given in Eq. (2.1) is valid for the experimentally relevant case of broad Feshbach resonances, where the effective range $r^\star$ of the resonant interaction is much smaller than the Fermi wavelength λ_F [4].

We consider a homogeneous situation described by a grand canonical distribution at fixed temperature and chemical potential. The grand partition function

$$Z = \mathrm{Tr}\{\exp(-\beta[\hat{H} - \mu\hat{N}])\} \quad (2.3)$$

then determines the grand potential

$$\Omega = \Omega(T, \mu) = -\beta^{-1} \ln Z. \quad (2.4)$$

For a quantitative discussion of the results, it is more convenient to switch to a canonical description at a given density n by a Legendre transformation to the free energy $F = \Omega + \mu N$. Within our zero-range interaction model, the Fermi system at total density $n = k_F^3/3\pi^2$ is then completely characterized by two parameters: the dimensionless temperature $\theta = k_B T/\varepsilon_F$ and the dimensionless inverse interaction strength $v = 1/k_F a$. In the special case of an infinite scattering length (the so-called unitarity limit), the parameter v drops out. The resulting spectral functions $A(\mathbf{k}, \varepsilon)$ are then universal functions of θ and the dimensionless momentum and energy scales k/k_F and $\varepsilon/\varepsilon_F$ that are set by the density of the gas.

A. Luttinger-Ward formalism

In thermal equilibrium at temperature T the properties of an interacting fermion system which exhibits a superfluid transition are described by two Matsubara Green's functions, the normal Green's function (T denotes the standard time ordering)

$$\langle T[\psi_\sigma(\mathbf{r}, \tau) \psi_{\sigma'}^+(\mathbf{r}', \tau')] \rangle = \delta_{\sigma\sigma'} \mathcal{G}(\mathbf{r} - \mathbf{r}', \tau - \tau') \quad (2.5)$$

and the anomalous Green's function

$$\langle T[\psi_\sigma(\mathbf{r}, \tau) \psi_{\sigma'}(\mathbf{r}', \tau')] \rangle = \varepsilon_{\sigma\sigma'} \mathcal{F}(\mathbf{r} - \mathbf{r}', \tau - \tau'), \quad (2.6)$$

where the antisymmetric Levi-Civita tensor $\varepsilon_{\sigma\sigma'}$ represents the spin structure of s-wave pairing. In the translation invariant and stationary case studied here, it is convenient to switch to a Fourier representation of the Matsubara Green's functions. The normal and anomalous functions (2.5) and (2.6) can then be combined into a matrix Green's function

$$G_{\alpha\alpha'}(\mathbf{k},\omega_n) = \begin{pmatrix} \mathcal{G}(\mathbf{k},\omega_n) & \mathcal{F}(\mathbf{k},\omega_n) \\ \mathcal{F}(\mathbf{k},\omega_n)^* & -\mathcal{G}(\mathbf{k},\omega_n)^* \end{pmatrix}, \qquad (2.7)$$

with momentum variable $\mathbf{k}$ and fermionic Matsubara frequencies $\omega_n = 2\pi(n+1/2)/\beta\hbar$ with $n \in \mathbb{Z}$. The nondiagonal elements represent the order parameter of the superfluid transition. Using matrix Green's function (2.7), it is possible to generalize the Luttinger-Ward formalism [27] to superfluid systems [21,26]. In particular, the grand thermodynamic potential (2.4) can be expressed as a unique functional of Green's function (2.7) in the form

$$\Omega[G] = \beta^{-1}\left(-\frac{1}{2}\text{Tr}\{-\ln G + [G_0^{-1}G - 1]\} - \Phi[G]\right). \qquad (2.8)$$

The interaction between the fermions is described by the functional $\Phi[G]$, which can be expressed in terms of a perturbation series of irreducible Feynman diagrams. The full matrix Green's function G is then determined uniquely by the condition that the grand potential functional (2.8) is stationary with respect to variations in G, i.e.,

$$\delta\Omega[G]/\delta G = 0. \qquad (2.9)$$

It is important to note that the thermodynamic potential $\Omega[G]$ is a functional of the exact Green's function G. The formalism of Luttinger and Ward thus leads via Eq. (2.9) to a self-consistent theory for the matrix Green's function.

Since the exact form of $\Phi[G]$ is unknown, we employ a ladder approximation [21,26,28]. In the weak-coupling limit, this is exactly equivalent to the standard BCS description of fermionic superfluids. In the BEC limit, where the fermions form a Bose gas of strongly bound pairs, the ladder approximation correctly accounts for the formation of pairs (i.e., the two-particle problem). The residual interaction between the pairs, however, is described only in an approximate manner. Indeed, it turns out [21,28] that in the BEC limit the ladder approximation for the functional $\Phi[G]$ gives rise to a theory for a dilute Bose gas with repulsive interactions that are described by a dimer-dimer scattering length $a_{dd}=2a$. This is a qualitatively correct description of the BEC limit of the crossover problem; however, from an exact solution of the four-particle problem in this limit the true dimer-dimer scattering length should be $a_{dd}=0.6a$ [29].

The ladder approximation leads to the following closed set of equations for the matrix of single-particle Green's functions (2.7) [21,26,28]:

$$G_{\alpha\alpha'}^{-1}(\mathbf{k},\omega_n) = G_{0,\alpha\alpha'}^{-1}(\mathbf{k},\omega_n) - \Sigma_{\alpha\alpha'}(\mathbf{k},\omega_n), \qquad (2.10)$$

$$\Sigma_{\alpha\alpha'}(\mathbf{k},\omega_n) = \Sigma_{1,\alpha\alpha'} + \int \frac{d^3K}{(2\pi)^3}\frac{1}{\beta}\sum_{\Omega_n}\Gamma_{\alpha\alpha'}(\mathbf{K},\Omega_n)$$
$$\times G_{\alpha'\alpha}(\mathbf{k}+\mathbf{K},\omega_n+\Omega_n), \qquad (2.11)$$

$$\Gamma_{\alpha\alpha'}^{-1}(\mathbf{K},\Omega_n) = \frac{\delta_{\alpha\alpha'}}{g} + \int \frac{d^3k}{(2\pi)^3}\left[\frac{1}{\beta}\sum_{\omega_n}G_{\alpha\alpha'}(\mathbf{k},\omega_n)\right.$$
$$\left.\times G_{\alpha\alpha'}(\mathbf{K}-\mathbf{k},\Omega_n-\omega_n) - \frac{m}{\hbar^2\mathbf{k}^2}\delta_{\alpha\alpha'}\right]. \qquad (2.12)$$

Here,

$$G_{0,\alpha\alpha'}^{-1}(\mathbf{k},\omega_n) = \begin{pmatrix} [-i\omega_n + \varepsilon_\mathbf{k} - \mu] & 0 \\ 0 & -[i\omega_n + \varepsilon_\mathbf{k} - \mu] \end{pmatrix} \qquad (2.13)$$

is the inverse free Green's function where $\varepsilon_\mathbf{k} = \hbar^2 k^2/2m$. Furthermore,

$$\Sigma_1 = \begin{pmatrix} 0 & \Delta \\ \Delta^* & 0 \end{pmatrix} \qquad (2.14)$$

is a $\mathbf{k}$- and ω_n-independent matrix, whose off-diagonal elements represent the order parameter of the superfluid transition. By definition, Δ is related to the anomalous Green's function $\mathcal{F}(\mathbf{k},\tau)$ by the renormalized gap equation

$$\Delta = g\int \frac{d^3k}{(2\pi)^3}\left[\mathcal{F}(\mathbf{k},\tau=0) + \Delta\frac{m}{\hbar^2\mathbf{k}^2}\right]. \qquad (2.15)$$

The vertex function $\Gamma_{\alpha\alpha'}(\mathbf{K},\Omega_n)$ defined in Eq. (2.12) may be identified with the T matrix for the scattering of two particles in a many-body Fermi system. Since $G_{\alpha\alpha'}(\mathbf{k},\omega_n)$ is the exact one-particle Green's function, the vertex function is that of a self-consistent T-matrix approximation. The Luttinger-Ward approach in ladder approximation is thus equivalent to a self-consistent T-matrix approximation. The specific structure of the GG term in Eq. (2.12) with respect to the Nambu indices α and α' implies that the particle-particle ladder is considered here, which properly describes the formation of Fermion pairs in normal and superfluid Fermi systems.

As a result of the Goldstone theorem, a neutral superfluid Fermi system must exhibit a gapless Bogoliubov-Anderson mode. Formally, this is guaranteed by a Ward identity, which can be derived from the Luttinger-Ward formalism for any gauge invariant functional $\Phi[G]$. This functional defines an associated inverse vertex function which in short-hand notation is given by

$$\Gamma^{-1} = \Gamma_1^{-1} + \chi, \qquad (2.16)$$

where $\Gamma_1 = -\delta^2\Phi[G]/\delta G^2$ is the irreducible vertex and $\chi = -GG$ is the pair propagator. The existence of a Bogoliubov-Anderson mode is then guaranteed by the property that Γ^{-1} has an eigenvalue $\lambda(\mathbf{K},\Omega_n)$ which has to vanish for $\mathbf{K}=0$ and $\Omega_n=0$ [26]. This Ward identity is equivalent, in the present case, to the well known Thouless criterion [30]. Unfortunately, the inverse vertex (2.12) obtained from our self-consistent ladder approximation does not agree with the exact inverse vertex function as defined by Eq. (2.16). As shown in our previous publication [21], however, the requirement of a gapless Bogoliubov-Anderson mode can be imposed on Eq. (2.12) as an additional constraint by choos-

ing a modified coupling constant in the renormalized gap Eq. (2.15). This modified approach is still compatible with the Luttinger-Ward formalism so that our method is both conserving and gapless. In the following numerical calculations we always employ this modified approach which is described in detail in Ref. [21].

In a homogeneous gas, the normal to superfluid transition is a continuous phase transition of the 3D *XY* type along the complete BCS to BEC crossover. By contrast, our approach [21] gives rise to a weak first-order superfluid transition because the superfluid phase of the Luttinger-Ward theory does not smoothly connect with the normal-fluid phase at a single critical temperature $\theta_c = k_B T_c / \varepsilon_F$. Fortunately, this problem is confined to a rather narrow regime of temperatures. In particular, at unitarity, the upper and lower values for θ_c are 0.1604 and 0.1506, which is within the present numerical uncertainties in the determination of the critical temperature of the unitary gas [31,32]. For our discussion of spectral functions in the present work, which does not focus on the critical behavior near T_c, the problem with the weak first-order nature of the transition is therefore not relevant.

Keeping these caveats in mind, the ladder approximation for the Luttinger-Ward functional provides quantitatively reliable results for the thermodynamic properties of the BCS-BEC crossover problem [21,22]. This applies, in particular, for the most interesting regime near unitarity, where weak-coupling approximations fail. As an example, the value of the critical temperature $T_c / T_F = 0.16$ right at unitarity agrees with recent quantum Monte Carlo (QMC) results $T_c / T_F = 0.152(7)$ for this problem within the error bars [31,32]. It is also consistent with recent calculations of the onset temperature of a finite condensate density [33]. Moreover, there is also quite good agreement with field-theoretic results for ground-state properties, which are characterized by a single universal constant, the so-called Bertsch parameter $\xi(0)$ defined, e.g., by $\mu(T=0) = \xi(0)\varepsilon_F$ at unitarity [4]. In fact, the value $\xi(0) = 0.36$ obtained within the Luttinger-Ward approach [21] agrees perfectly with the result $\xi(0) = 0.367(9)$ from an $\epsilon = 4-d$ expansion up to three loops [34] and—in particular—with the more recent value $\xi = 0.36 \pm 0.002$ obtained by Nishida [35]. Variational Monte Carlo calculations [36,37] or a Gaussian fluctuation expansion around the BCS mean-field results [38,39], in turn, give somewhat higher values $\xi(0) = 0.42(1)$ or $\xi(0) = 0.40$, respectively.

B. Spectral functions

The Matsubara Green's function $\mathcal{G}(\mathbf{k}, \omega_n)$ can be expressed in terms of a spectral function $A(\mathbf{k}, \varepsilon)$ by using the Lehmann spectral representation [40]

$$\mathcal{G}(\mathbf{k}, \omega_n) = \int d\varepsilon \frac{A(\mathbf{k}, \varepsilon)}{-i\hbar\omega_n + \varepsilon - \mu}. \tag{2.17}$$

The spectral function associated with the normal, single-particle Green's function $\mathcal{G}(\mathbf{k}, \omega_n)$ is positive $A(\mathbf{k}, \varepsilon) \geq 0$ and normalized according to

$$\int d\varepsilon A(\mathbf{k}, \varepsilon) = 1. \tag{2.18}$$

It can be decomposed into two contributions

$$A(\mathbf{k}, \varepsilon) = A_+(\mathbf{k}, \varepsilon) + A_-(\mathbf{k}, \varepsilon), \tag{2.19}$$

which describe the particle and hole excitation part of the complete excitation spectrum. The individual contributions

$$A_+(\mathbf{k}, \varepsilon) = Z^{-1} \sum_{mn} e^{-\beta(E_m - \mu N_m)} |\langle m|\psi_\sigma(\mathbf{0})|n\rangle|^2 (2\pi)^3$$
$$\times \delta(\mathbf{k} - [\mathbf{P}_n - \mathbf{P}_m]/\hbar)\delta(\varepsilon - [E_n - E_m]) \tag{2.20}$$

and

$$A_-(\mathbf{k}, \varepsilon) = Z^{-1} \sum_{mn} e^{-\beta(E_n - \mu N_n)} |\langle m|\psi_\sigma(\mathbf{0})|n\rangle|^2 (2\pi)^3$$
$$\times \delta(\mathbf{k} - [\mathbf{P}_n - \mathbf{P}_m]/\hbar)\delta(\varepsilon - [E_n - E_m]) \tag{2.21}$$

can be expressed in terms of matrix elements of single fermion field operators $\psi_\sigma(\mathbf{0})$ at the origin between the exact eigenstates $|n\rangle$ of the many-body system. Here $\mathbf{P}_n$, E_n, and N_n are the corresponding eigenvalues of momentum, energy, and particle number, respectively. In thermal equilibrium, the partial spectral functions are related by the detailed balance condition

$$A_-(\mathbf{k}, \varepsilon) = e^{-\beta(\varepsilon - \mu)} A_+(\mathbf{k}, \varepsilon). \tag{2.22}$$

At zero temperature, therefore, the hole part $A_-(\mathbf{k}, \varepsilon)$ of the spectral function vanishes for $\varepsilon > \mu$ and vice versa the particle part $A_+(\mathbf{k}, \varepsilon)$ vanishes for $\varepsilon < \mu$. The total spectral weight in the hole part

$$\int d\varepsilon A_-(\mathbf{k}, \varepsilon) = n_\sigma(\mathbf{k}) \tag{2.23}$$

at arbitrary temperatures is equal to the fermion occupation number $n_\sigma(\mathbf{k}) = -\mathcal{G}(\mathbf{k}, \tau = -0)$ for a single spin orientation σ (in the balanced gas discussed here, both components $\sigma = \pm 1$ have the same occupation, of course).

Within the BCS description of fermionic superfluids, the spectral function consists of two infinitely sharp peaks [40]

$$A(\mathbf{k}, \varepsilon) = u_\mathbf{k}^2 \delta(\varepsilon - E_\mathbf{k}^{(+)}) + v_\mathbf{k}^2 \delta(\varepsilon - E_\mathbf{k}^{(-)}), \tag{2.24}$$

which represent the particle and hole part of the spectral function. The associated energies

$$E_\mathbf{k}^{(\pm)} = \mu \pm \sqrt{(\varepsilon_\mathbf{k} - \mu)^2 + \Delta^2} \tag{2.25}$$

describe the standard dispersion of the Bogoliubov quasiparticles. They exhibit a finite gap, whose minimum value Δ is taken at a finite momentum $k_\mu = \sqrt{2m\mu}/\hbar$ (note that $\mu \to \varepsilon_F > 0$ in the BCS limit). Within the standard BCS theory, these excitations have infinite lifetime at arbitrary momenta $\mathbf{k}$ and there is no broadening or incoherent background. Going beyond the exactly solvable BCS Hamiltonian, however, gives rise to a finite lifetime of the fermionic excitations and thus will broaden the two delta peaks in Eq. (2.24) even at zero

temperature. It is our aim in the following to calculate these effects quantitatively for the simple model Hamiltonian Eq. (2.1) in the whole range of coupling strengths and temperatures.

Equation (2.17) has the form of a Cauchy integral in the theory of complex functions. It is therefore convenient to define a complex Green's function $G(\mathbf{k}, z)$ depending on a complex frequency z, which is analytic in the upper and lower complex half planes $\mathrm{Im}(z) \gtrless 0$, respectively. This complex Green's function is related the Matsubara Green's function and to the spectral function by

$$\mathcal{G}(\mathbf{k}, \omega_n) = G(\mathbf{k}, z = \mu/\hbar + i\omega_n), \qquad (2.26)$$

$$A(\mathbf{k}, \varepsilon) = \pm \pi^{-1} \mathrm{Im}[G(\mathbf{k}, z = \varepsilon/\hbar \pm i0)], \qquad (2.27)$$

respectively. Thus, in a first step we obtain the complex Green's function $G(\mathbf{k}, z)$ as an analytic continuation from the Matsubara Green's function $\mathcal{G}(\mathbf{k}, \omega_n)$. In a second step, we insert the complex frequency $z = \varepsilon/\hbar \pm i0$ and obtain the spectral function $A(\mathbf{k}, \varepsilon)$ from Eq. (2.27). The fact that $\mathcal{G}(\mathbf{k}, \omega_n)$ uniquely determines the spectral function has been proven by Baym and Mermin [41].

In practice the analytic continuation for calculating the spectral function $A(\mathbf{k}, \varepsilon)$ is done by using the maximum-entropy method [42] which is described in detail in Appendix A. We have checked the accuracy of our results *a posteriori* by inserting the calculated spectral functions in Eq. (2.17). The given "initial" data $\mathcal{G}(\mathbf{k}, \omega_n)$ are then found to be reproduced with a relative accuracy that is typically in the 10^{-5} range.

C. rf response

In radio-frequency experiments, the external rf field transfers atoms from one of the two occupied spin states (as initial state) into an empty final state. In the following, we assume that the final state, which is denoted by an index f, has a negligible interaction with the initial one. It can thus be described by the free-fermion spectral function

$$A_f(\mathbf{k}, \varepsilon) = \delta(\varepsilon - [E_f + \varepsilon_{\mathbf{k}}]), \qquad (2.28)$$

where E_f is the excitation energy of the final state, which has a free particle dispersion $\varepsilon_{\mathbf{k}} = \hbar^2 k^2 / 2m$. Within linear response, the rate of transitions out of the initial state induced by the rf field with frequency ω and wave vector $\mathbf{q}$ is given by a convolution

$$I(\mathbf{q}, \omega) = \hbar \int \frac{d^3k}{(2\pi)^3} \int d\varepsilon [A_{f,+}(\mathbf{k} + \mathbf{q}, \varepsilon + \hbar\omega)A_-(\mathbf{k}, \varepsilon)$$
$$- A_{f,-}(\mathbf{k} + \mathbf{q}, \varepsilon + \hbar\omega)A_+(\mathbf{k}, \varepsilon)] \qquad (2.29)$$

of the spectral functions A and A_f of the initial and final states. Here, an unknown prefactor that depends on the interaction parameters for the coupling to the rf field has been set equal to $\hbar$, which provides a convenient normalization for the total weight integrated over all frequencies [see Eq. (2.36) below]. This overall constant drops out in normalized spectra by dividing out the zeroth moment $\int d\omega I(\mathbf{q}, \omega)$ or has—in any case—to be adjusted to the measured signal in

comparison with experimental data. Since the wave vector $\mathbf{q}$ of the rf field is much smaller than those of the atoms, it is an excellent approximation to set $\mathbf{q} = 0$. In the absence of a probe that selects atoms according to their momenta $\mathbf{k}$, the spectrum $I(\mathbf{q} = 0, \omega) = I(\omega)$ is thus only a function of the rf frequency ω. In addition, for the standard situation with an empty final state f, the partial spectral functions are $A_{f,+}(\mathbf{k}, \varepsilon) = A_f(\mathbf{k}, \varepsilon)$ and $A_{f,-}(\mathbf{k}, \varepsilon) = 0$. Using Eq. (2.28), the resulting rf spectrum

$$I(\omega) = \hbar \int \frac{d^3k}{(2\pi)^3} A_-(\mathbf{k}, \varepsilon_{\mathbf{k}} - \hbar\omega) \qquad (2.30)$$

is an integral over the hole part $A_-(\mathbf{k}, \varepsilon)$ of the single-particle spectral function in the initial strongly correlated state. For convenience we have taken $E_f = 0$, which redefines the position of zero frequency $\omega = 0$ in the rf spectrum.

Within a BCS description, the spectral function is given by Eq. (2.24). Its hole excitation part has a delta peak at $E_{\mathbf{k}}^{(-)}$ whose weight is equal to the occupation number $n_\sigma(\mathbf{k}) = v_{\mathbf{k}}^2$. This reflects the simple fact that a hole with momentum $\mathbf{k}$ can only be created if a fermion is present with this momentum. The resulting rf spectrum in our normalization is

$$I_{BCS}(\omega) = \frac{m^{3/2}}{2^{1/2}\pi^2\hbar^2} \left[\frac{\hbar\omega}{2} + \mu - \frac{\Delta^2}{2\hbar\omega} \right]^{1/2} \frac{\Delta^2}{2(\hbar\omega)^2}. \qquad (2.31)$$

It exhibits a sharp onset at $\hbar\omega_{min} = \sqrt{\Delta^2 + \mu^2} - \mu$. As will be shown below, such a sharp onset is not found from our numerical results for the spectral function even in the weak-coupling limit $v \ll -1$. The origin of this discrepancy may be traced back to the fact that the dominant contributions to the rf spectrum near ω_{min} arise from the spectral function $A_-(\mathbf{k}, \varepsilon)$ in the limit $\mathbf{k} \to 0$, i.e., far from the Fermi surface at k_F. Now, deep in the Fermi sea, the true spectral function is not described properly by an extended BCS description, which has sharp quasiparticles at *arbitrary* momenta. In fact, the simple form (2.24) of the single fermion spectral function holds only if the interaction part of the full Hamiltonian Eq. (2.1) is approximated by the exactly soluble reduced BCS Hamiltonian [43]. Its interaction term

$$\hat{H}'_{BCS} = \frac{g_0}{2V} \sum_\sigma \sum_{\mathbf{k}, \mathbf{k}'} c^+_{\mathbf{k}, \sigma} c^+_{-\mathbf{k}, -\sigma} c_{-\mathbf{k}', -\sigma} c_{\mathbf{k}', \sigma} \qquad (2.32)$$

involves only pairs with vanishing total momentum $\mathbf{Q} = 0$. This approximation excludes density fluctuations and therefore does not account for the collective Bogoliubov-Anderson mode [4]. Moreover, its fermionic quasiparticles are exact eigenstates of the reduced BCS Hamiltonian at arbitrary momenta. The difference

$$\hat{H}_{res} = \frac{g_0}{2V} \sum_\sigma \sum_{\mathbf{k}, \mathbf{k}', \mathbf{Q} \neq 0} c^+_{\mathbf{k}+\mathbf{Q}, \sigma} c^+_{-\mathbf{k}, -\sigma} c_{-\mathbf{k}', -\sigma} c_{\mathbf{k}'+\mathbf{Q}, \sigma} \qquad (2.33)$$

between the full Hamiltonian Eq. (2.1) and that of the reduced BCS model therefore gives rise to residual interactions between the quasiparticles and their coupling to the collec-

tive Bogoliubov-Anderson mode. This will be discussed in more detail in Appendix B. As will be shown quantitatively in Sec. IV, the residual interactions result in an appreciable broadening $\gamma(\mathbf{k})$ of the spectral functions. In particular, the hole part becomes increasingly broad as $\mathbf{k} \to \mathbf{0}$ [see Fig. 2(a) for a coupling strength $v = -1$]. A BCS-type rf spectrum (2.31) requires that $\gamma(\mathbf{k}=\mathbf{0}) \ll \hbar\omega_{min} \approx \Delta^2/2\varepsilon_F$ in weak coupling. This condition is never fulfilled in practice, because the gap $\Delta \sim \exp(\pi v/2)$ vanishes exponentially in the BCS limit $v \ll -1$, while $\gamma(\mathbf{k}=\mathbf{0})$ can be shown to be of order $(k_F a)^2$ as $k_F|a| \ll 1$ due to the decay via intermediate states involving three quasiparticles [see Eq. (B8) in Appendix B]. As a result, the onset and peak shift of the rf spectrum in weak coupling are dominated by the Hartree contributions and do not reflect the appearance of a pairing gap.

In the limit $v \gg +1$ of a molecular BEC, the fermions form a superfluid of strongly bound dimers. In this regime, the gap parameter Δ becomes negligible compared with the magnitude of the chemical potential and hole excitation energy (2.25) approaches $E_{\mathbf{k}}^{(-)} \to 2\mu - \varepsilon_{\mathbf{k}}$. Since the extended BCS description of the crossover becomes exact again in the molecular limit, where it reduces to an ideal Bose gas of dimers, one can use Eq. (2.24) for the associated spectral function of fermionic excitations, which gives

$$A_-(\mathbf{k}, \varepsilon) = v_{\mathbf{k}}^2 \delta(\varepsilon + \varepsilon_{\mathbf{k}} - 2\mu) \qquad (2.34)$$

in the BEC limit. The weight $v_{\mathbf{k}}^2 = 4\pi n a^3 (1 + \mathbf{k}^2 a^2)^{-2}$ now coincides with the square of the bound state wave function in momentum space. The resulting rf spectrum

$$I_{BEC}(\omega) = \frac{n}{\pi a \sqrt{m}} \frac{(\hbar\omega + 2\mu)^{1/2}}{\omega^2} \qquad (2.35)$$

is a special case of that derived by Chin and Julienne [44] in the molecular limit for bound-free transitions in the absence of final state interactions. It has an onset $\hbar\omega_{min,BEC} = -2\mu \to \varepsilon_b$ that is determined by the molecular binding energy $\varepsilon_b = \hbar^2/ma^2$ as expected. This energy also sets the scale for the half width of the rf spectrum, which is $E_w = \gamma\varepsilon_b$ with a numerical factor $\gamma = 1.89$.

D. rf spectra at high frequencies and contact density

Our definition of the rf spectrum in Eq. (2.30) and normalization (2.23) of the hole part of the spectral function imply that the total weight integrated over all frequencies

$$\int d\omega\, I(\omega) = n_\sigma = n/2 \qquad (2.36)$$

is determined by the density n_σ of atoms from which the transfer to the empty final state f occurs. This normalization fixes the overall prefactor and determines the normalized form of the rf spectra in which the zeroth moment is divided out. An analysis of the spectra in terms of their nontrivial higher moments, however, does not seem to work. Indeed, it follows from Eqs. (2.31) and (2.35) that the rf spectra at high frequencies fall off like $\omega^{-3/2}$ both in the BCS and the BEC limit. Thus, already the first moment of the spectrum diverges. The issue of the behavior at high frequencies has

been investigated recently by Schneider *et al.* [45]. They have shown that the exact expression (2.30) quite generally implies an $\omega^{-3/2}$ power-law decay

$$I(\omega \to \infty) = \frac{C}{4\pi^2} \left(\frac{\hbar}{m}\right)^{1/2} \omega^{-3/2}. \qquad (2.37)$$

Here, the coefficient C is defined by the behavior $n_\sigma(k) \to C/k^4$ of the momentum distribution at large momenta. It was introduced by Tan [23] as a parameter that characterizes quite generally fermionic systems with zero-range interactions. As shown by Braaten and Platter [24], this coefficient is a measure of the probability that two fermions with opposite spin are close together and is thus called a contact density or simply the contact. In the balanced superfluid, it has actually been determined from a measurement of the closed channel fraction by Partridge *et al.* [46], as analyzed in detail by Werner *et al.* [47]. In the BEC limit, the well known expression for $n_\sigma(k)$ in terms of the square of the bound state wave function yields $C_{BEC} = 4\pi n/a$, consistent with the explicit form (2.35) of the spectrum in the BEC limit.

There are two important points in this context, which we discuss in the following. First of all, the asymptotic $\omega^{-3/2}$ power-law decay of the exact rf spectrum is valid only in the ideal case of zero-range interactions and identically vanishing final state effects. Indeed, an explicit calculation of the rf spectrum in the molecular limit by Chin and Julienne [44] shows that in the presence of a nonzero scattering length $a_f \neq 0$ between the hyperfine state that is not affected by the rf pulse and the final state of the rf transition, the spectrum decays like $\omega^{-5/2}$ at large frequencies. The short-range part of the interaction, which is responsible for the slow decay of the spectrum, is therefore cancelled out by the interaction between the final state and the state that remains after the rf transition. This result remains valid quite generally along the whole BCS-BEC crossover as discussed by Zhang and Leggett [48,49]. In particular, this behavior guarantees that the rf spectrum has a finite first moment. As shown in Refs. [12,13], it allows to define an average "clock shift"

$$\hbar\bar{\omega} = s\frac{4\varepsilon_F^2}{n_\sigma}\left(\frac{1}{g} - \frac{1}{g_f}\right) \qquad (2.38)$$

that is again determined by the contact coefficient $C = sk_F^4$ and the renormalized interaction constants $g = 4\pi\hbar^2 a/m$ and $g_f = 4\pi\hbar^2 a_f/m$. In particular, there is a perfect "atomic peak" $I(\omega) \sim \delta(\omega)$ and no clock shift at all if $a = a_f$. The existence of higher moments of the rf spectrum relies on accounting for the nonzero range $r_0 \neq 0$ of the interaction. Since this is expected to affect the spectrum only at frequencies of order $\hbar/mr_0^2$, this regime, however, will hardly be accessible experimentally.

As a second point, we consider the behavior of the contact coefficient C in the weak-coupling limit. Standard BCS theory for the momentum distribution at large k predicts that the corresponding dimensionless factor $s = C/k_F^4$ is exponentially small, $s_{BCS} = (\Delta/2\varepsilon_F)^2$. This is in agreement with the high frequency asymptotics of the ideal BCS spectrum (2.31) without final state interactions according to the result in Eq. (2.37).

It turns out, however, that the exponentially small value of the contact coefficient in the BCS limit is an artifact of working with a reduced BCS Hamiltonian, which only takes into account pairing part (2.32) of the interaction. By contrast, the full Hamiltonian gives an additional contribution that is associated with noncondensed close pairs. For weak coupling, this is much larger than that of the condensed pairs described by the BCS theory. More precisely, it turns out that the coefficient

$$s = [\Delta^2 - \Gamma_{11}(\mathbf{r} = \mathbf{0}, \tau = -0)]/(4\varepsilon_F^2) \qquad (2.39)$$

in front of the $n_\sigma(k) = s(k_F/k)^4$ behavior of the momentum distribution at large k contains a nontrivial contribution associated with the upper diagonal element Γ_{11} of the vertex function defined in Eq. (2.12) in the limit of vanishing spatial and temporal separation. In the molecular limit, the contribution from this term is negligible. The asymptotic result $\Delta_{BEC} = 2\varepsilon_F\sqrt{4v/3\pi}$ for the gap parameter then gives rise to a linearly increasing dimensionless contact parameter $s_{BEC} = 4v/3\pi$ consistent with the naive result discussed above. On the contrary, in the weak-coupling limit, the contribution from noncondensed close pairs is dominant compared with the exponentially small BCS contribution from condensed pairs. In the limit $v \ll -1$ the leading behavior is given by

$$-\Gamma_{11}(\mathbf{0}, -0) = \left(\frac{4\varepsilon_F}{3\pi v}\right)^2. \qquad (2.40)$$

The resulting dimensionless contact coefficient $s_{wc} = (2/3\pi v)^2$ in weak coupling is therefore much larger than the exponentially small BCS contribution. It is remarkable that the leading term in the weak-coupling contact density of the superfluid with $a < 0$ is identical to the one that is obtained in a *repulsive* dilute normal Fermi liquid with $a > 0$, which has first been calculated by Belyakov [50]. This shows that the dominant contribution to the contact density is independent of the sign of the interaction consistent with the "adiabatic theorem"

$$\frac{\partial u}{\partial(1/a)} = -\frac{\hbar^2}{4\pi m} C(a) \qquad (2.41)$$

that relates the derivative of the energy per volume u with respect to the inverse scattering length to the contact coefficient C [24,51]. In fact, the simple mean-field interaction energy linear in a, which is the leading correction to the ground-state energy of the ideal Fermi gas, shows that $C(a) \sim a^2$ is independent of the sign of interactions to lowest order. The BCS pairing effects, that appear in the case of a negative scattering length, only give a subdominant, exponentially small reduction in the energy that is reflected in a corresponding tiny enhancement of the contact density. The full dependence of $s(v)$ along the BCS to BEC crossover for the balanced gas at zero temperature is shown in Fig. 1. The particular value $s(0) = 0.098$ at unitarity has in fact been determined before in the context of the average clock shift (2.38) [12] and is close to our present value $s(0) = 0.102$ that follows from Eq. (2.39). Since the contact density is a short-range correlation property, it is not very sensitive to temperature; see [52].
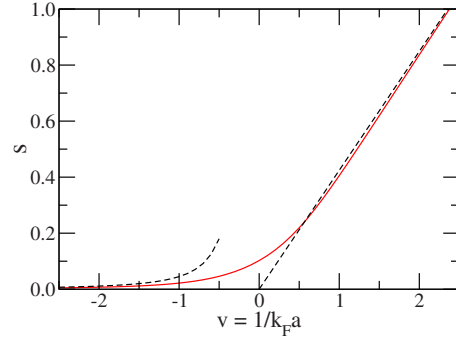

FIG. 1. (Color online) The dimensionless contact coefficient s is shown as a function of the dimensionless coupling strength $v = 1/k_F a$. The red solid line represents our numerical result obtained from Eq. (2.39). The left and right black dashed lines represent the asymptotic formulas s_{wc} and s_{BEC} given in the text, respectively.

An important consequence of the failure of naive BCS theory to account for the correct value of the contact density C in weak coupling is the fact that the weight of the rf spectrum at high frequencies that is determined by Eq. (2.37) in the absence of final state interactions or by the average clock shift (2.38) is strongly underestimated by using the idealized form (2.24) of the spectral functions that follow from a naive BCS theory. It is an interesting open problem to determine analytically the explicit form of the spectral functions in the weak-coupling limit which is consistent with the correct high frequency asymptotics (2.37) with the proper value for the contact density.

III. EFFECTIVE-FIELD THEORY AND PAIR SIZE

For a molecular BEC that consists of tightly bound dimers, the notion of a pair size is well defined. In the relevant case of a zero-range two-particle interaction with positive scattering length a, it is determined by the rms extension $\xi_m = a/\sqrt{2}$ of the two-body bound state. Since $k_F a \ll 1$ in the BEC limit, the size of the pairs in this regime is much smaller than the average interparticle spacing $(3\pi^2)^{1/3}/k_F \approx 3.1/k_F$ of the fermionic gas in the absence of an attractive interaction. Motivated by the fact that rf spectroscopy in this limit effectively reduces to a two-body molecular spectrum, a spectroscopic pair size ξ_w has been determined from the half width of the measured rf spectrum $I(\omega)$ by the relation $\xi_w^2 = \gamma \times \hbar^2/2mE_w$ [18]. By its definition, this pair size coincides with the molecular size $\xi_m = a/\sqrt{2}$ in the appropriate limit. Extending this definition to arbitrary coupling strengths, one obtains a ground-state pair size $\xi_w = 0.86\hbar v_F/\Delta_0$ in the opposite BCS limit, which correctly describes the exponentially large size of Cooper pairs characteristic for weak-coupling BCS superconductors [53]. It is thus plausible to use this spectroscopic definition of the pair size for the complete range of couplings, in particular also near the unitarity limit [18]. The measured rf spectrum at the lowest temperature, that has been reached experimentally, is then found to give an effective pair size $\xi_w \simeq 2.6/k_F$ at unitarity [18]. This is somewhat smaller than the average inter-

particle spacing indicating that the unitary gas has pairs that no longer overlap. The numerical value for the pair size is in fact close to that obtained from calculating the width of the pair wave function in a variational ansatz for the ground state of the BCS-BEC crossover [54].

An obvious question in this context is whether there are independent measures of the pair size which do not rely on the spectroscopic definition that is motivated by the extrapolation from the molecular limit or on the related variational approximation for the ground state in terms of a product of two-body wave functions. In the following, we will show that a many-body definition of the pair size can be obtained from the q-dependent superfluid response function following the basic concept of a nonlocal penetration depth in superconductors [53]. This response can be calculated from an effective-field theory of the superfluid state including the next-to-leading order corrections to the standard quantum hydrodynamic Lagrangian. Remarkably, the value of the pair size at unitarity that follows from the q-dependent superfluid response is close to that inferred spectroscopically from the half width of the rf spectrum.

The basic idea that allows to define a characteristic length ξ_p of a fermionic superfluid without reference to an approximate BCS or molecular description of the many-body ground state is related to the well known calculation of the q-dependent penetration depth $\lambda(q)$ in charged superconductors. The latter is defined by the nonlocal generalization $\mathbf{j}(q) = -\mathbf{A}(q)/4\pi\lambda^2(q)$ of the London equation relating the current density induced by a transverse vector potential in linear response [53]. The square of the inverse effective penetration depth determines the superfluid density $n_s(q)$, which obeys $n_s(q=0) = n$ in any Galilei invariant superfluid. For finite momentum q the superfluid response is reduced by a correction that has to vanish like q^2 in an isotropic system. The correction defines a characteristic length ξ_p according to

$$n_s(q) = n\left(1 - \frac{\pi^2}{30}q^2\xi_p^2 + \cdots\right) \tag{3.1}$$

in the limit of small wave vectors q. Here, the prefactor in the q^2 correction has been chosen in such a way that the characteristic length ξ_p coincides with the Pippard length $\xi_P = \hbar v_F/\pi\Delta_0$ in the weak-coupling limit.

In order to determine the value of ξ_p at unitarity, one needs the leading order corrections in an expansion in small gradients to the universal quantum hydrodynamic Lagrangian density

$$\mathcal{L}_0 = \frac{\hbar^2 n}{2m}\left[\frac{1}{c_s^2}\dot\varphi^2 - (\nabla\varphi)^2\right] \tag{3.2}$$

of a translation invariant, neutral superfluid with (Bogoliubov-Anderson) sound velocity c_s. For the unitary Fermi gas, where $c_s^2 = 2\mu/3m$ exactly, these corrections have been discussed in detail by Son and Wingate [25]. Restricting ourselves to the harmonic description of the Goldstone mode described by Eq. (3.2) to leading order, the next-to-leading terms in the effective-field theory are of the form [25]

$$\mathcal{L}' = \hbar\left[c_1\sqrt{\frac{m}{\mu}}(\nabla\dot\varphi)^2 + c_2\sqrt{\frac{\mu}{m}}(\nabla^2\varphi)^2\right]. \tag{3.3}$$

The associated dimensionless coefficients $c_{1,2}$ can only be determined from a microscopic theory. Their physical meaning becomes evident from the fact that c_2 determines the reduction of the superfluid response for finite wave vectors q as described in Eq. (3.1). In terms of the pair size ξ_p defined there, one finds

$$\frac{\pi^2}{30}\xi_p^2 = 9c_2\frac{\sqrt{m\mu}}{\hbar n}, \tag{3.4}$$

which also makes clear that c_2 has to be positive. In contrast to c_2, the coefficient c_1 has no direct physical interpretation. From the plane-wave solution of the linear equations of motion for the phase fluctuations that follow from the total Lagrangian density $\mathcal{L}_0 + \mathcal{L}'$ it is easy to see, however, that this coefficient appears in the next-to-leading corrections in the dispersion $\omega(q) = c_s q(1 - aq^2/k_F^2 + \cdots)$ of the Bogoliubov-Anderson mode with a dimensionless coefficient [25]

$$a = \pi^2\sqrt{2\xi(0)}\left(\frac{3}{2}c_2 + c_1\right). \tag{3.5}$$

Here $\xi(0) \approx 0.36$ is the Bertsch parameter, which relates the sound and bare Fermi velocities by $c_s^2 = \xi(0)v_F^2/3$. Similar to the Bertsch parameter, which appears in the leading order Lagrangian (3.2), the coefficients $c_{1,2}$ can be calculated in an expansion around the upper critical dimension four of the unitary Fermi gas as suggested originally by Nussinov and Nussinov [55] and started by Nishida and Son [56]. A one-loop calculation of the coefficients $c_{1,2}$ has recently been performed by Rupak and Schäfer [57]. The resulting value of c_1 at $\epsilon = 4 - d = 1$ turns out to be $c_1 \approx -0.02$. Unfortunately, for c_2, the one-loop calculation is not sufficient, because a finite value of c_2 only appears at order ϵ^2 [57]. This is easy to understand from connection (3.4) between c_2 and the pair size, which is expected to vanish linearly in $\epsilon = 4 - d$. Indeed in four dimensions, a two-particle bound state in a zero-range potential only appears at infinitely strong attraction [55]. The unitary gas in $d = 4$ therefore has a vanishing dimer size and is effectively an ideal Bose gas similar to the situation in the BEC limit in $d = 3$ [58]. In order to fix the value of c_2 for the unitary gas in three dimensions, we use connection (3.5) between the next-to-leading order coefficients of the effective-field theory and the q^3 corrections to the dispersion $\omega(q)$ of the Bogoliubov-Anderson mode. This dispersion has been calculated within a Gaussian fluctuation approximation for arbitrary coupling strengths v [39] and exhibits a negative curvature with $a \approx 0.06$ right at unitarity [59]. Combined with the value of c_1 from the ϵ expansion, this leads to the estimate $c_2 \approx 0.02$ for the unitary gas in three dimensions. As a result, the pair size that follows from Eq. (3.4) turns out to be $\xi_p \approx 2.62/k_F$. It is remarkable that this value essentially coincides with that inferred from the spectroscopic definition in Ref. [18] or the width of the pair wave function in Ref. [54]. It should be noted, though, that apart from the uncertainties in the precise values of $c_{1,2}$, there is a certain amount of arbitrariness in defining a "pair size," both from the rf
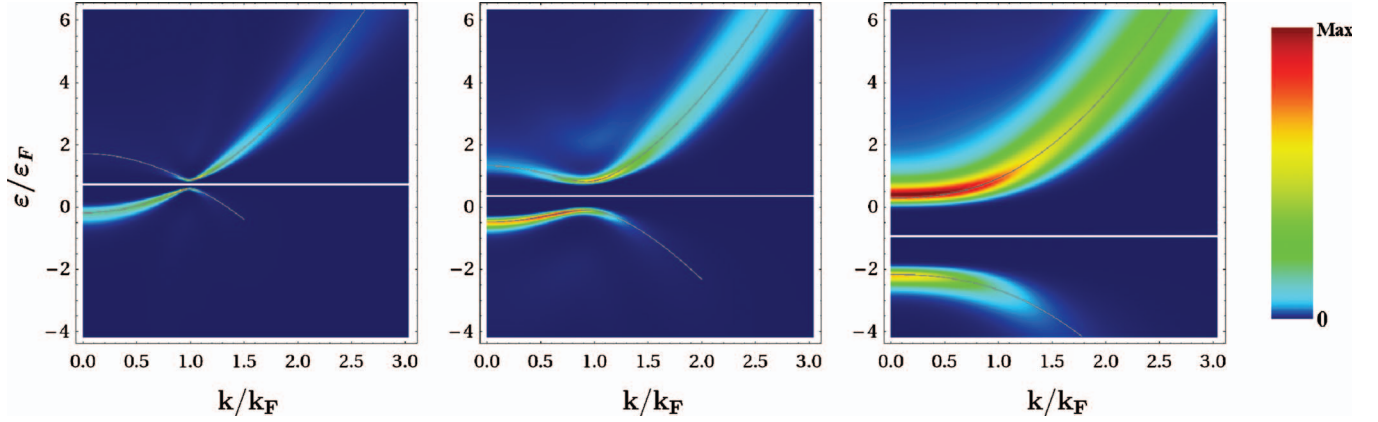
FIG. 2. (Color) Density plots of the spectral function $A(k, \varepsilon)$ at temperature $T=0.01T_F$ for the interaction strengths $v = 1/(k_F a) = -1, 0,$ $+1$ from left to right. The white horizontal lines indicate the chemical potential μ. The gray lines are fits to the maxima of $A(\mathbf{k}, \varepsilon)$ using Eq. (4.1).

spectrum or from the q-dependent superfluid response via Eq. (3.4). This is related to the precise choice of the prefactor both in the spectroscopic definition and in Eq. (3.4), where the Pippard length has been used as a reference scale. The naive conclusion that the unitary gas has nonoverlapping pairs in its ground state should therefore be viewed with a great deal of caution.

The fact that the coefficients $c_{1,2}$ of the next-to-leading order Lagrangian (3.3) have a comparable magnitude at unitarity has a further interesting consequence. Indeed, these coefficients determine the magnitude of the Weizsäcker inhomogeneity correction [60,61]

$$\varepsilon_W(x) = b \frac{\hbar^2}{2m} \frac{[\nabla n(x)]^2}{n(x)} \qquad (3.6)$$

to the ground-state energy density of the unitary Fermi gas [57]. The associated dimensionless coefficient b is related to the q^2 corrections of the density response [25]

$$\chi(q) = \chi(0) \left[1 - b \left(\frac{\hbar q}{mc_s} \right)^2 + \cdots \right]. \qquad (3.7)$$

For the unitary Fermi gas, the coefficient b is again determined by the next-to-leading order Lagrangian (3.4) via [57]

$$b = \frac{32\pi^2}{3} [\sqrt{2\xi(0)}]^3 \left(\frac{9}{2} c_2 - c_1 \right). \qquad (3.8)$$

Using our estimates for $c_{1,2}$, this leads to $b \approx 0.22$, a value that is almost one order of magnitude larger than the result $b^{(0)} = 1/36 = 0.028$ which is obtained for an ideal Fermi gas. The unitary gas is therefore remarkable in the sense that its kinetic energy density $\varepsilon_{kin}(x) \sim \xi(0) n^{5/3}(x)$ is *reduced* by the Bertsch parameter $\xi(0) \approx 0.36$ compared with the noninteracting gas, yet the coefficient b of the Weizsäcker inhomogeneity correction is strongly *enhanced* [57].

IV. NUMERICAL RESULTS

In the following, we present numerical results for the spectral function $A(\mathbf{k}, \varepsilon)$ and the rf spectrum $I(\omega)$ which can

be compared with experimental data. The numerical calculations are performed in two steps. First, the Matsubara Green's function $\mathcal{G}(\mathbf{k}, \omega_n)$ is calculated by solving the self-consistent Eqs. (2.10)–(2.15). In a second step the spectral function $A(\mathbf{k}, \varepsilon)$ is calculated from Eq. (2.17) by analytical continuation as described in Sec. II B. For this purpose we employ a maximum-entropy method that is described in Appendix A. Eventually, the rf spectrum $I(\omega)$ is calculated by evaluating momentum integral (2.30) numerically.

A. Spectral functions

Our numerical results for the spectral functions $A(\mathbf{k}, \varepsilon)$ in the experimentally relevant range of interaction strengths $v = -1, 0,$ and $+1$ are shown in Fig. 2. The associated temperature is $T = 0.01T_F$, i.e., deep in the superfluid regime in all three cases. Evidently, both at $v = -1$ and at unitarity $v = 0$, a BCS-like quasiparticle structure appears with an excitation gap whose minimum is at a finite value of the momentum. On the BEC side, at $v = +1$, the backbending in the dispersion curve has apparently disappeared. This is consistent with the expected existence of a critical value $v_s > 0$, beyond which the fermionic excitations have their minimum at $\mathbf{k} = 0$. From our numerical data on the momentum dependence of the fermionic excitation spectrum, the associated critical coupling constant is $v_s = 0.8$. This is about a factor of 2 larger than the mean-field prediction, which is determined by the zero crossing of the chemical potential. The fact that v_s occurs in the regime where the chemical potential is already negative has been noted before in an $\varepsilon = 4 - d$ expansion by Nishida and Son [62]. Extrapolating their one-loop result to $\varepsilon = 1$ gives $\mu_s \simeq -0.5\varepsilon_F$ at the critical coupling v_s in rather good agreement with our result $\mu_s \simeq -0.54\varepsilon_F$. In population imbalanced gases the change in the curvature of the fermionic excitation spectrum at v_s determines the critical coupling of the splitting point S at which the continuous transition from a balanced to an imbalanced superfluid on the BEC side splits into two first-order transitions [63].

Empirically, the form of the quasiparticle dispersion relations may be extracted from the peak position of the spectral

TABLE I. Effective mass m^* and Hartree shift U of the quasiparticle dispersion relations at $T=0.01T_F$ obtained by fitting Eq. (4.1) to the peak maxima of the spectral functions in Fig. 2.

v	μ/ε_F	Δ/ε_F	Particle		Hole	
			m^*/m	U/ε_F	m^*/m	U/ε_F
−1	0.73	0.14	1.05	−0.26	1.12	−0.17
0	0.36	0.46	1.00	−0.50	1.19	−0.35
+1	−0.93	1.10	1.02	−0.42	1.28	−0.37

function. It turns out that these peaks fit reasonably well to a modified dispersion

$$\widetilde{E}_{\mathbf{k}}^{(\pm)} = \mu \pm \sqrt{\left(\frac{m}{m^*}\varepsilon_{\mathbf{k}} + U - \mu\right)^2 + \Delta^2} \qquad (4.1)$$

of Bogoliubov quasiparticles, in which the effective mass m^* and an additional Hartree shift U are used as fit parameters. The associated values for m^* and U that follow from the spectral functions shown in Fig. 2 are summarized in Table I. It is interesting to note that both the masses and the Hartree shifts are different for particle and hole excitations. The particle-hole symmetry of the standard BCS description of the quasiparticle dispersion is therefore broken at these large coupling strengths. A second feature of interest is that the hole dispersion relation $E_{\mathbf{k}}^{(-)}$ starts to deviate from BCS form (4.1) only for momenta $k \gtrsim 1.5k_F$, when the spectral weight of the hole peak is smaller than 0.5%.

Using QMC methods, the particle dispersion relation at unitarity and $T=0$ has been calculated previously by Carlson and Reddy [64]. Our values for the Hartree shift U and the effective mass m^* of the particle dispersion relation agree reasonably well with the QMC values. Experimentally, the Hartree shift U was extracted recently from rf measurements by Schirotzek *et al.* [65]. In this work, the measured peak positions of the rf spectra were fitted with the peak position obtained from BCS formula (2.31) including an additional Hartree shift: $\omega_{\mathrm{peak}}^{BCS}=4[\sqrt{(\mu-U)^2+15\Delta^2/16}-\mu+U/4]/3$. If we apply this method to our calculated rf spectra, we obtain different values for U than those listed in Table I. In particular, this method gives $U=-0.28,-0.52,-0.22$ for $v=-1,0,$ $+1$ at $T=0.01T_F$ and does not take the effective mass into account (we note that the rf spectrum is only sensitive to the hole excitation part of the spectral function). This discrepancy is probably due to the fact that the assumption of having sharp quasiparticles is not reliable in this regime.

It is evident from the quantitative form of the spectral functions that the parametrization of the fermionic excitations by a modified dispersion (4.1) is not an adequate description of the excitation spectrum because of the rather strong broadening of the quasiparticle peaks even at very low temperatures. The physical origin of this broadening is the residual interaction between the quasiparticles that follows from the Hamiltonian in Eq. (2.33). As shown in Appendix B, this interaction leads to a finite width of the spectral functions even at $T=0$, except near the minimum of the dispersion curve for the particle excitations and close to the maximum of the dispersion for the hole excitations. Here, the

quasiparticle lifetime broadening has to vanish because there are no available final states into which it may decay. Focusing on the interaction of the quasiparticles with the collective Bogoliubov-Anderson mode, which is the dominant mechanism for decay near the minimum (maximum) of the particle (hole) dispersion curve, it is straightforward to see that there is actually a finite interval in momentum space where the spectral width vanishes identically. This width is determined by the kinematic constraint that that the quasiparticle decay by emission of phonons is possible only if the group velocity $\partial E_{\mathbf{k}}/\partial \mathbf{k}$ of the fermionic excitations becomes larger than the sound velocity c_s. In fact a similar situation appears for a hole in a Néel-ordered antiferromagnet, whose spectral function is sharp as long as its group velocity is below the spin-wave velocity of antiferromagnetic magnons [66]. The fact that our numerically calculated spectral functions $A(\mathbf{k},\varepsilon)$ exhibit a finite broadening at the lowest temperature $T=0.01T_F$ even near the dispersion minimum is probably related both to the numerical procedure of evaluating $A(\mathbf{k},\varepsilon)$ using the Maxent technique which can never give rise to perfectly sharp peaks, but also to the self-consistent structure of our Luttinger-Ward formulation. Indeed, in a diagrammatic language, the latter implies summation of diagrams with identical intermediate states for fermions, which—in an exact theory—are excluded by the Pauli principle. Unfortunately, to our knowledge, there exist no analytical results on the broadening of the Bogoliubov quasiparticles beyond the perturbative treatment outlined in Appendix B. Experimentally, this question may in principle be resolved by studying momentum-resolved rf spectra that have recently been obtained by Stewart *et al.* [19]. Unfortunately, at present, experimental data on spectral functions are available only near the critical temperature of the superfluid transition, where the finite lifetime arises due to the scattering with thermally excited quasiparticles.

To discuss the situation at finite temperature, we plot the spectral function $A(\mathbf{k},\varepsilon)$ at unitarity for different temperatures above and below T_c in Figs. 3 and 4. It is interesting to observe how the two BCS-like quasiparticle peaks evolve with increasing temperature and finally merge into a single excitation structure with a quadratic dispersion at temperatures around T_c. Note, however, that the spectral peak in the normal phase is shifted to negative energies compared to the free fermion dispersion relation $\varepsilon_{\mathbf{k}}=\hbar^2\mathbf{k}^2/2m$. This Hartree shift is responsible for the observation of shifts in experimentally measured rf spectra above T_c, which will be discussed in detail below. The observation of such a shift in the rf spectra in the normal state is therefore not necessarily a signature of pseudogap effects.
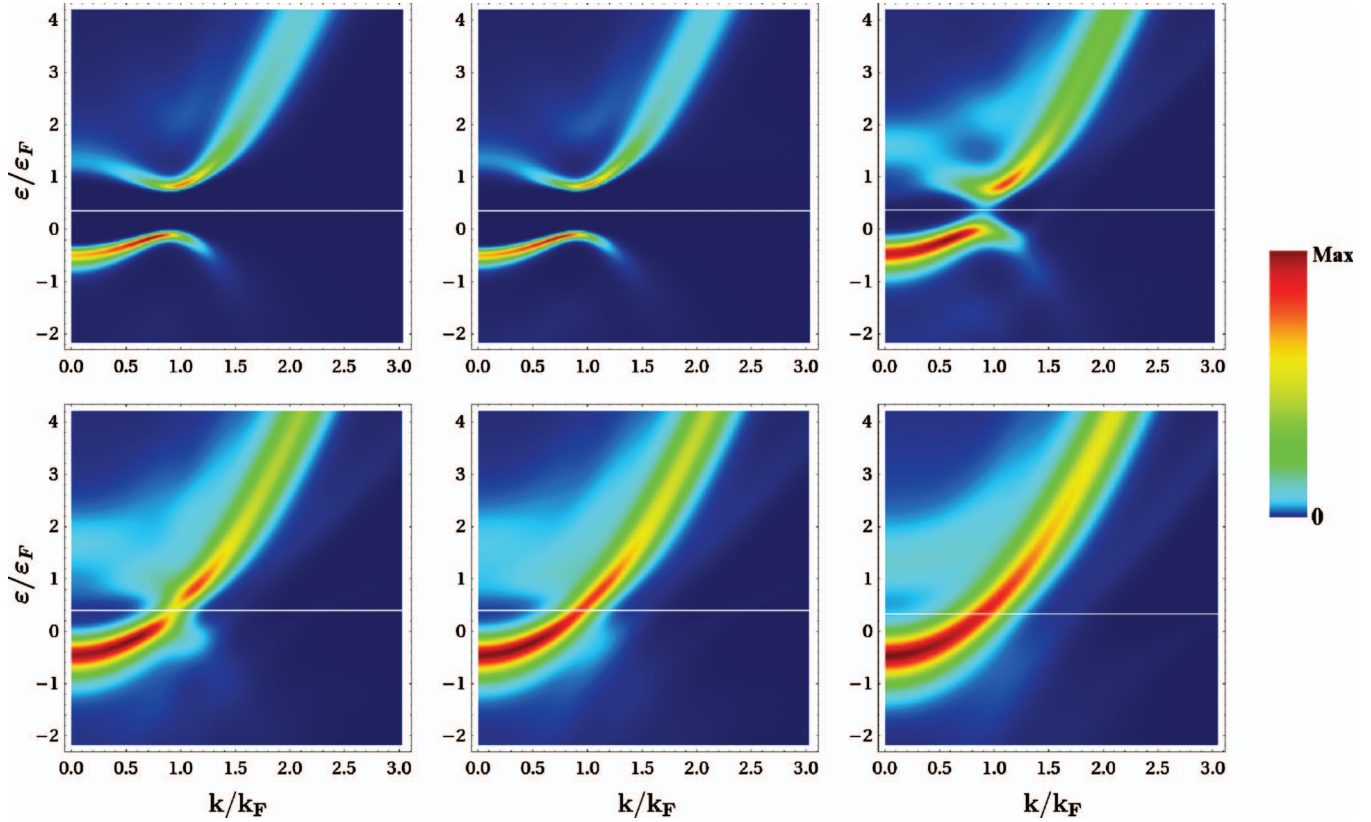
FIG. 3. (Color) Density plots of the spectral function $A(\mathbf{k}, \varepsilon)$ at unitarity $[v = 1/(k_F a) = 0]$ for different temperatures. From top left to bottom right: $T/T_F = 0.01$, 0.06, 0.14, $0.160(T_c)$, 0.18, and 0.30. The white horizontal lines mark the chemical potential μ. At temperatures smaller than the superfluid transition temperature T_c two quasiparticle structures with a BCS-like dispersion can be seen. The width of the spectral peaks is of the same order as the quasiparticle energy. With increasing temperature the two branches gradually merge into a single quasiparticle structure with a quadratic dispersion above T_c. Note, however, that the quadratic dispersion is shifted to negative frequencies compared to the bare fermion dispersion relation. This Hartree shift is of the order of $U = -0.46\varepsilon_F$ and is essentially responsible for the shifted rf spectra in the normal phase in Fig. 6.

Finite temperature QMC calculations of the spectral function at unitarity by Bulgac *et al.* [67] indicate the presence of a gapped particle excitation spectrum of form (4.1) also
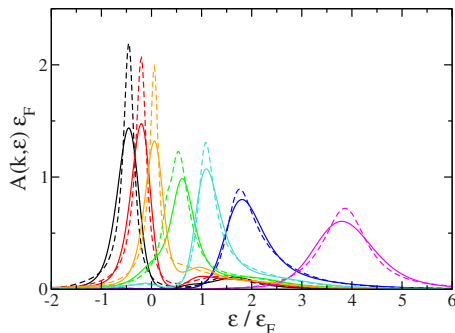

FIG. 4. (Color online) The spectral function $A(\mathbf{k}, \varepsilon)$ as a function of ε for selected fixed values k at unitarity $v = 1/(k_F a) = 0$ and at criticality $T/T_F = 0.160(T_c)$. The selected values of the wave number k are represented by the colors of the lines corresponding to the peaks from left to right: $k/k_F = 0.00$ (black), 0.52 (red), 0.77 (orange), 1.00 (green), 1.26 (cyan), 1.51 (blue), and 2.02 (magenta). The different methods for calculating the spectral function are distinguished by the line styles: maximum-entropy method (solid lines) and Padé approximation (dashed lines).

above the critical temperature, which is not found in our approach. More generally, it is evident from the spectral functions of the unitary gas above T_c which are shown in Fig. 3 that a simple pseudogap ansatz for the spectral function [69] is not consistent with our results. As can be seen from the lower three graphs in Fig. 3, our approach leads to a single, broad, ungapped excitation peak with a quadratic dispersion at temperatures $T > T_c$ instead of two excitation branches with a gapped BCS-like dispersion as expected from the pseudogap approach. In particular we do not observe a strong suppression of spectral weight near the chemical potential.

Apart from the dominant peaks discussed above our spectral functions show some additional structures that have much smaller weight, however. Specifically, at unitarity and temperatures above T_c a small second peak is visible for $k \lesssim k_F$ in Fig. 3. At $T = 0.3T_F$ this residual peak contains $\sim 17\%$ of the spectral weight. The situation is similar on the BEC side of the Feshbach resonance at $v = 1$, where above T_c a second peak at negative energies is present for $k \lesssim k_F$, with a spectral weight of $\sim 22\%$.

Recent experiments by Stewart *et al.* [19] have succeeded to perform rf spectroscopy in a momentum-resolved manner from which one directly obtains the hole spectral function $A_-(\mathbf{k}, \varepsilon)$ as a function of both momentum and energy. A
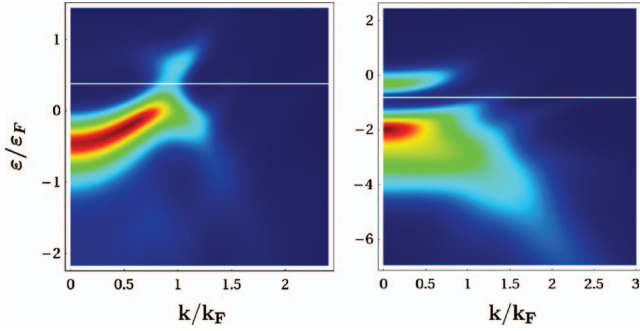
FIG. 5. (Color) Density plot of the hole part of the spectral function $A_-(\mathbf{k},\varepsilon)$ at unitarity $v=1/(k_Fa)=0$ and $T/T_F=0.150$ slightly below T_c (left) and in the BEC regime at $v=1/(k_Fa)=+1$ and $T/T_F=0.207$ at the superfluid transition temperature (right). The white horizontal line marks the chemical potential μ. The color scheme is the same as in Figs. 2 and 3.

quantitative comparison with our calculated spectral functions is difficult, however, since the measured spectral functions involve an average over the inhomogeneous density profile of the trapped atoms. Nevertheless, as shown in Fig. 5, the qualitative structure of our hole spectral function of the uniform system near the critical temperature is similar to that observed experimentally. To separate the intrinsic from an inhomogeneous broadening in a trap requires combining momentum and local resolution, which is currently investigated in the group at JILA. Experiments of this kind would allow to distinguish between different models for the spectral functions, in particular for the "pseudogap" phase immediately above T_c. The existence of preformed pairs in this regime is often described by sharp spectral functions of form (2.24) with a nonvanishing gap parameter Δ_{pg}. As shown recently by Chen *et al.* [70] and Dao *et al.* [71], this assumption is also consistent with present experimental data due to the inhomogeneous averaging associated with the position-dependent gap parameter in a trap.

B. rf response

In Fig. 6 we show the calculated rf spectra together with the locally resolved experimental data of Schirotzek *et al.* [65] from MIT. The measured rf data shown in Fig. 6 have been corrected for the small mean-field final state interaction energy, which allows for a direct comparison with our calculated spectra. For a detailed comparison we must take the finite experimental resolution into account, however. Schirotzek *et al.* use an approximately rectangular rf pulse with a length of $T=200$ μs in order to transfer atoms to the empty hyperfine state. Thus, the Fourier spectrum of the radio-frequency source has a finite width and the calculated spectra obtained using Eq. (2.30) need to be convolved with $\mathrm{sinc}^2(\omega T/2)$, i.e.,

$$I_{\exp}(\omega) = \int d\omega' I(\omega-\omega')\mathrm{sinc}^2(\omega' T/2). \qquad (4.2)$$

The finite experimental resolution thus leads to a slight broadening and a small shift to higher frequencies of the
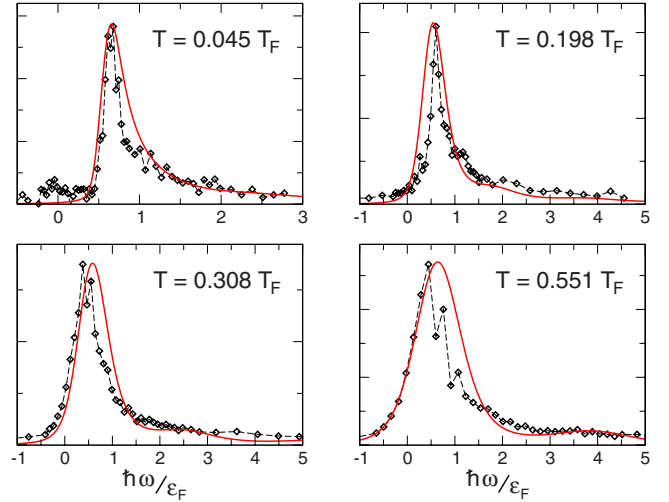

FIG. 6. (Color online) Comparison of the calculated rf spectra at unitarity with the experimental data of Schirotzek *et al.* [65] from MIT at different temperatures T. Our numerical result is shown by the red solid line. The experimental data are represented by open diamonds connected by straight thin dashed lines. Apart from adjusting the peak heights, no fitting parameters have been used.

calculated rf spectra. At unitarity and $T=0.01T_F$, the broadening is $\sim 0.07\varepsilon_F$ and the shift $\sim 0.01\varepsilon_F$.

As can be seen in Fig. 6, the rf spectra in the homogeneous system show a single peak that is shifted compared to the bare transition frequency, which is set to $\omega=0$ for convenience. Apart from slightly overestimating the width of the spectral lines, our numerically obtained spectra agree very well with the experimental data. Note that no fitting parameters have been used apart from adjusting the absolute height.

In the first rf measurements by Chin *et al.* [10] a secondary peak at the bare transition frequency has been observed and attributed to the presence of unpaired atoms. In these experiments, however, the measurement of the spectra involved an average over the inhomogeneous density profile of the trapped atoms. Since more recent locally resolved rf measurements [17] did not show signs of an atomic peak, it is likely that these peaks either originate from the low density regions at the edge of the atomic cloud or are an effect of the strong final state interactions.

It is important to notice that there are essentially two contributions to the rf peak shift. The first one is due to pairing correlations, which are particularly important in the superfluid phase and give the dominant contribution to the peak shift on the BEC side of the crossover, where the fermions are paired in two-body bound states. The second contribution comes from Hartree-type correlations. The Hartree contribution dominates the peak shift in the normal phase, where pairing correlations are small. Furthermore, it also dominates in the BCS regime, since the gap is exponentially small whereas the Hartree contribution scales linearly with k_Fa. Together with the discussion of the residual interaction between the quasiparticles in Sec. II C this implies that BCS formula (2.31) for the rf spectrum in weak coupling is completely misleading.

V. DISCUSSION

The results presented above on the spectral functions and the associated rf spectra of ultracold fermionic gases near a Feshbach resonance have two major aspects. First of all, they provide a quantitative description of recent experiments on the excitation spectra of the near unitary gas. The theory covers the complete range of temperatures from the superfluid near zero temperature to the anomalous normal state above T_c which is characterized by strong pairing fluctuations. From a theoretical point of view, our results are of relevance as a simple example, where the standard quasiparticle description of BCS theory is strongly modified. As a result of interactions between quasiparticles and their coupling to the collective Bogoliubov-Anderson phonon, the spectral functions acquire a finite broadening even at zero temperature except for a small range of momenta around the dispersion minimum (maximum) of the particle (hole) excitations. Effectively, the fermionic excitations along the BCS-BEC crossover are not a Fermi gas as in BCS theory but are described by a Fermi-liquid picture. The spectral functions therefore have vanishing width at zero temperature at a sharply defined surface in momentum space, where the excitation energy has its minimum [68]. Within a perturbative calculation around the BCS limit, this has been shown explicitly in Appendix B. More generally, it is expected to be valid for arbitrary coupling because the phase space for quasiparticle decay vanishes near the dispersion minimum. We are not aware, however, of a general proof of this statement for the simple model (2.1) of attractively interacting fermions studied here.

As discussed in Sec. II C, the finite lifetime of the fermionic excitations at small momenta is particularly important for the onset of the rf spectra shown in Fig. 6. In the BCS picture, where the spectral function has vanishing width at arbitrary momentum **k**, the rf spectra would exhibit a sharp onset. As argued above, however, the fermionic excitations near **k**=0 have a finite width even at $T=0$ up to the critical coupling v_s because they are far away from the maximum of the hole dispersion. As a result, the rf spectra have no sharp onset in agreement with the experimental observation. A further important aspect of our results is that the naive description of the BCS-BEC crossover problem by an extended BCS ansatz [4], that appears to work qualitatively at least for the ground state, is completely inadequate as far as dynamical correlations are concerned. In particular, the simple form of the spectral function in Eq. (2.24) that follows from a naive BCS theory is never valid because the pure pairing Hamiltonian on which it is based misses both the broadening, e.g., due to collective excitations, and the large contribution to the contact coefficient due to noncondensed close pairs. A rather surprising conclusion of our work is that the next-to-leading terms in the effective-field theory for the Bogoliubov-Anderson mode allow us to give a many-body definition of the pair size which agrees quite well with the result found experimentally from the half width of the rf spectrum.

There are of course a number of open problems which should be addressed in future work. In particular, it would be interesting to understand to which extent the normal phase above T_c can be understood in terms of a pseudogap model, which has been applied with reasonable success to understand angle-resolved photoemission spectroscopy experiments in the context of high T_c cuprates [69]. As far as pseudogap effects are concerned, our spectral functions close to T_c show a different behavior than previous non-self-consistent calculations [72–74] and more recent QMC calculations [67], which exhibit a pseudogap. Quite generally it is known that non-self-consistent calculations favor pseudogap behavior, whereas self-consistent calculations suppress pseudogap effects (cf. [75] and references therein). We emphasize, however, that in the context of ultracold gases, the available momentum and energy resolution in experiments at present is not good enough to map out the spectral function in sufficient detail. Apart from the rather good agreement between the observed rf spectra and our results for the underlying spectral function, the confidence that our self-consistent Luttinger-Ward approach to the BCS-BEC crossover gives quantitatively reliable results is supported by the very precise description it provides for thermodynamic properties (see the discussion at the end of Sec. II A) much better than non-self-consistent approaches. It is an open problem to determine spectral functions, e.g., from QMC data, at the level of accuracy that has now been achieved for equilibrium properties.

APPENDIX A: MAXIMUM-ENTROPY METHOD

In order to solve Eq. (2.17) explicitly for $A(\mathbf{k}, \varepsilon)$ the integral is discretized. We chose equally spaced energies ε in the inner interval $-10\varepsilon_F < \varepsilon < +10\varepsilon_F$ and logarithmically spaced energies in the outer regions $-10^6\varepsilon_F < \varepsilon < -10\varepsilon_F$ and $+10\varepsilon_F < \varepsilon < +10^6\varepsilon_F$. We evaluate the integral by using the trapezoid formula. On the right-hand side of Eq. (2.17) the Matsubara Green's function $\mathcal{G}(\mathbf{k}, \omega_n)$ is given for selected Matsubara frequencies $\omega_n^{(l)}$ on a logarithmic scale, which are ordered according to $0 < \omega_n^{(1)} < \omega_n^{(2)} < \cdots < \omega_n^{(l_{max})} \sim 10^6\varepsilon_F$. In this way, Eq. (2.17) is transformed into a set of linear equations which can be solved by standard numerical methods.

Unfortunately, the linear equations are nearly singular even if the number of discrete energies ε (number of un-

known variables) is smaller than l_{max} (number of equations). Many eigenvalues of the linear matrix are very close to zero, so that small numerical errors in the Matsubara Green's function $\mathcal{G}(\mathbf{k}, \omega_n)$ are enhanced exponentially. As a result, the spectral function $A(\mathbf{k}, \varepsilon)$ cannot be calculated by this simple method.

In order to improve and stabilize the method we need some prior information. We assume that a smooth backgroundlike prior spectral function $A_0(\varepsilon)$ is given. We define the *entropy*

$$S(\mathbf{k}) = \int d\varepsilon \{A(\mathbf{k}, \varepsilon) - A_0(\varepsilon) - A(\mathbf{k}, \varepsilon)\ln[A(\mathbf{k}, \varepsilon)/A_0(\varepsilon)]\},$$

$$(\text{A1})$$

where the integral is evaluated numerically by the trapezoid formula for the above defined discrete energies ε. The spectral function $A(\mathbf{k}, \varepsilon)$ is obtained by maximizing the entropy (A1) for given wave vectors $\mathbf{k}$ where Eq. (2.17) is used as a constraint. This procedure is known as the maximum-entropy method and can be derived by Bayes inference [76]. It has been applied successfully for calculating the spectral function $A(\mathbf{k}, \varepsilon)$ from the Matsubara Green's function $\mathcal{G}(\mathbf{k}, \omega_n)$ in Monte Carlo simulations [42].

In order to implement the constraints we define the chi square

$$[\chi(\mathbf{k})]^2 = \frac{1}{l_{max}} \sum_{l=1}^{l_{max}} |d(\mathbf{k}, \omega_n^{(l)})|^2/\sigma^2, \qquad (\text{A2})$$

where

$$d(\mathbf{k}, \omega_n) = -i\hbar\omega_n \left[\mathcal{G}(\mathbf{k}, \omega_n) - \int d\varepsilon \frac{A(\mathbf{k}, \varepsilon)}{-i\hbar\omega_n + \varepsilon - \mu} \right]$$

$$(\text{A3})$$

is a dimensionless difference and σ is a dimensionless standard deviation. Minimizing $[\chi(\mathbf{k})]^2$ we recover the constraint equations (2.17).

By solving the self-consistent equations of Sec. II we calculate the Matsubara Green's function $\mathcal{G}(\mathbf{k}, \omega_n)$ with a relative accuracy of about 10^{-5}. For this reason, we expect $|d(\mathbf{k}, \omega_n)| \sim 10^{-5}$ and chose the fixed value $\sigma = 10^{-5}$ for the standard deviation. As a result we observe $\chi(\mathbf{k}) \sim 1$ in our numerical calculations where variations occur by a factor of 10 for different wave vectors $\mathbf{k}$.

Using Bayes inference [76] it can be shown that

$$Q(\mathbf{k}) = \alpha S(\mathbf{k}) - \frac{1}{2}[\chi(\mathbf{k})]^2 \qquad (\text{A4})$$

is the functional which must be maximized by variation in the spectral function $A(\mathbf{k}, \varepsilon)$ for every fixed wave vector $\mathbf{k}$. The related necessary condition is

$$\frac{\delta Q(\mathbf{k})}{\delta A(\mathbf{k}, \varepsilon)} = 0, \qquad (\text{A5})$$

which implies the equations to be solved numerically for $A(\mathbf{k}, \varepsilon)$. In Eq. (A4) α is a Lagrange parameter which

balances the weight between entropy (A1) and constraints (A2). For $\alpha = 0$ we recover constraint equations (2.17). On the other hand, in the limit $\alpha \to \infty$ we obtain the prior spectral function $A(\mathbf{k}, \varepsilon) = A_0(\varepsilon)$. Thus, α is a parameter which must be adjusted to an intermediate value in order to obtain an optimum result for the spectral function $A(\mathbf{k}, \varepsilon)$. For low values α the constraints are overweighted. A more accurate result is obtained for $A(\mathbf{k}, \varepsilon)$; however, instabilities may occur. On the other hand, for higher values α the entropy is overweighted. A more stable result is obtained which, however, may be less accurate.

We have defined entropy (A1) and chi square (A2) as dimensionless quantities which are of order unity. For this reason, we expect that α must be of order unity, too. Actually, we find that $\alpha = 1$ is an optimum choice in most areas of the phase diagram except for low temperatures. For this reason, we use $\alpha = 1$ in most cases. However, for low temperatures $T \lesssim 0.5 T_c$ the spectral function $A(\mathbf{k}, \varepsilon)$ is very close to zero in the gap region. Since the numerical algorithm considers the logarithm $\ln[A(\mathbf{k}, \varepsilon)]$ an instability occurs. Hence, in this latter case for low temperatures we choose $\alpha = 100$ in the crossover and BEC regime, and $\alpha = 1000$ in the BCS regime.

For the success of the method an appropriate choice for the prior spectrum $A_0(\varepsilon)$ is very important. First of all the prior spectrum $A_0(\varepsilon)$ should be a smooth function of the energy ε which models a broad background spectrum. The special form of entropy (A1) does *not* require $A_0(\varepsilon)$ to be normalized. Constraint equations (2.17) will determine the spectral function $A(\mathbf{k}, \varepsilon)$ for small and intermediate energies in the inner interval $-10\varepsilon_F \lesssim \varepsilon \lesssim +10\varepsilon_F$. However, the constraints will provide less information in the tail regions $\varepsilon \ll -10\varepsilon_F$ and $\varepsilon \gg +10\varepsilon_F$. For this reason our method is considerably improved if the prior spectrum $A_0(\varepsilon)$ already shows the correct wings for $\varepsilon \to \pm\infty$.

Investigating the Matsubara Green's function for large Matsubara frequencies $\omega_n \to \pm\infty$ we obtain the asymptotic formula

$$\mathcal{G}(\mathbf{k}, \omega_n) \approx (-i\hbar\omega_n)^{-1} + a_{\mathbf{k}}(-i\hbar\omega_n)^{-2} + \pi b(-i\hbar\omega_n)^{-5/2},$$

$$(\text{A6})$$

where $a_{\mathbf{k}} = -(\varepsilon_{\mathbf{k}} - \mu)$ and $b = (2/3\pi^2)(2\varepsilon_F)^{3/2}$. The analytic continuation by substitution $i\hbar\omega_n \to \hbar z - \mu$ yields the asymptotic complex Green's function

$$G(\mathbf{k}, z) \approx (-\hbar z)^{-1} - \varepsilon_{\mathbf{k}}(-\hbar z)^{-2} + \pi b(-\hbar z)^{-5/2} \quad (\text{A7})$$

for $|z| \to \infty$. Eventually from Eq. (2.27) we obtain the asymptotic spectral function $A(\mathbf{k}, \varepsilon) \approx b\theta(\varepsilon)\varepsilon^{-5/2}$ for $\varepsilon \to \pm\infty$. Thus, the weight of the asymptotic power law of the spectral function is described by the constant factor b which is real, positive, and independent of $\mathbf{k}$.

A prior spectrum which meets all these requirements and which shows the correct wings is given by

$$A_0(\varepsilon) = b \frac{[\varepsilon^2 + \gamma^2]^{1/2} + \varepsilon}{2[\varepsilon^2 + \gamma^2]^{7/4}}. \qquad (\text{A8})$$

The denominator represents a modified Lorentz spectrum with a nontrivial exponent. In order to have a smooth func-

tion, we choose a large spectral width $\gamma = 20\varepsilon_F$. The specific form of the numerator and the exponent of the denominator guarantee the correct wings for $\varepsilon \to \pm \infty$ in leading order. It turns out that the prior spectrum $A_0(\varepsilon)$ can be chosen independent of **k**.

In our implementation of the method we solve Eq. (A5) numerically by using Bryan's algorithm [77]. The rectangular matrix of the discretized constraint equations (2.17) is decomposed by using a singular-value decomposition. Eventually we observe that only a small fraction of about 15–20 eigenvalues provide essential contributions for the spectral function $A(\mathbf{k}, \varepsilon)$.

The maximum-entropy method must be applied for each value of the wave vector **k** in order to obtain the complete spectral function $A(\mathbf{k}, \varepsilon)$. We find that the parameters of the method σ, α, γ, and b can be chosen independent of **k**. We observe that entropy (A1) together with the prior spectrum (A8) guarantees a positive spectral function $A(\mathbf{k}, \varepsilon) > 0$. Finally, in our numerical calculations we observe that the dimensionless difference (A3) has the same order $\sim 10^{-5}$ over the whole range of Matsubara frequencies ω_n and for all **k** which is essential for the quality of our implementation of the maximum-entropy method.

APPENDIX B: LIFETIME OF FERMIONIC EXCITATIONS AT ZERO TEMPERATURE

In this appendix we outline an analytical calculation of the lifetime of fermionic excitations at zero temperature, which is perturbative in deviations from the exactly soluble reduced BCS Hamiltonian (2.32). For arguments that indicate a breakdown of well-defined fermionic excitations in the opposite BEC limit see [78].

Quite generally a quasiparticle description of the BCS-BEC crossover problem requires that the low lying excitations above the exact ground state with energy E_0 can be described by a noninteracting gas of quasiparticles,

$$H = E_0 + \sum_q \omega_\mathbf{q} b_\mathbf{q}^\dagger b_\mathbf{q} + \sum_{\mathbf{k},\sigma} \widetilde{E}_\mathbf{k} \alpha_{\mathbf{k}\sigma}^\dagger \alpha_{\mathbf{k}\sigma}. \quad \text{(B1)}$$

The first term accounts for the Bogoliubov-Anderson phonons with linear dispersion $\omega_\mathbf{q} = c_s q$ for momenta **q** that are small compared to the inverse healing length. The second term describes the fermionic excitations which have a gapped spectrum $\widetilde{E}_\mathbf{k}$. The crucial requirement that the lifetime of the quasiparticles by far exceeds their energy is trivially fulfilled for the bosonic excitations. In the weak-coupling BCS regime their lifetime is actually infinite up to an energy 2Δ, which is necessary for a decay into two fermionic quasiparticles. On the BEC side they can decay through nonlinear corrections to the quantum hydrodynamic Lagrangian (3.2). Provided that the curvature parameter a introduced in Sec. III is negative, this leads to a width $\sim q^5$ by Beliaev damping, which is negligible in the $\mathbf{q} \to 0$ limit.

Regarding the fermionic quasiparticles, their lifetime turns out to be infinite near the dispersion minimum despite the fact that their excitation energy becomes of the order of the Fermi energy in the experimentally relevant regime near a Feshbach resonance. At unitarity, for instance, the zero-

temperature gap is $\Delta = 0.46\varepsilon_F$ [21] in very good agreement with recent quantum Monte Carlo results [79]. The fermionic spectral function should therefore exhibit a sharp peak near the dispersion minimum at zero temperature. Indeed, the relevant process that limits the lifetime close to the dispersion minimum is the emission of a Bogoliubov-Anderson phonon with momentum **q**. Due to energy and momentum conservation, this process must obey the kinematic constraint

$$E_\mathbf{k} = E_{\mathbf{k}-\mathbf{q}} + c_s |\mathbf{q}|, \quad \text{(B2)}$$

where **k** is the initial momentum of the fermionic excitation with dispersion $E_\mathbf{k} = \mu + \sqrt{(\varepsilon_\mathbf{k} - \mu)^2 + \Delta^2}$ and c_s is the sound velocity. Equation (B2) implies that the emission of a phonon is impossible as long as the group velocity of the fermionic excitations is smaller than the sound velocity $|\partial E_\mathbf{k} / \partial \mathbf{k}| < c_s$. This condition is always true for a small interval of momenta around the dispersion minimum implying that the lifetime of a fermionic excitation is infinite in this region.

In the following we show briefly how the kinematic constraint (B2) arises, if the residual interaction (2.33) between BCS quasiparticles is taken into account perturbatively. Our starting point is a reformulation of BCS-BEC crossover Hamiltonian (2.1) in terms of BCS quasiparticle operators. The reduced BCS Hamiltonian (2.32) can be diagonalized exactly [43,80] and takes the form

$$H_{BCS} = E_0^{BCS} + \sum_{\mathbf{k},\sigma} E_\mathbf{k} \alpha_{\mathbf{k}\sigma}^\dagger \alpha_{\mathbf{k}\sigma}. \quad \text{(B3)}$$

It has the form of the more general quasiparticle Hamiltonian (B1), but is actually valid at arbitrary momenta and energies. However, it misses completely the Bogoliubov-Anderson phonons. The quasiparticle operators $\alpha_{\mathbf{k}\sigma}$ are related to the fermionic operators $c_{\mathbf{k}\sigma}$ via the usual Bogoliubov transformation

$$c_{\mathbf{k}\uparrow} = u_\mathbf{k} \alpha_{\mathbf{k}\uparrow} + v_\mathbf{k} \alpha_{-\mathbf{k}\downarrow}^\dagger, \quad \text{(B4)}$$

$$c_{-\mathbf{k}\downarrow} = -v_\mathbf{k} \alpha_{\mathbf{k}\uparrow}^\dagger + u_\mathbf{k} \alpha_{-\mathbf{k}\downarrow}, \quad \text{(B5)}$$

with the coefficients $u_k^2 = [1 + (\varepsilon_\mathbf{k} - \mu)/(E_\mathbf{k} - \mu)]/2$ and $v_k^2 = [1 - (\varepsilon_\mathbf{k} - \mu)/(E_\mathbf{k} - \mu)]/2$. The ground state is determined by the condition $\alpha_{\mathbf{k}\sigma}|GS\rangle = 0$. Before proceeding, we mention that the lifetime of the fermionic excitations is directly related to the lifetime of the BCS quasiparticles, since the fermionic Green's function $G(\mathbf{k}, \omega)$ can be expressed in terms of the BCS quasiparticle Green's function $\mathcal{G}(\mathbf{k}, \omega)$ as

$$G_\sigma(\mathbf{k}, \omega) = u_k^2 \mathcal{G}_\sigma(\mathbf{k}, \omega) - v_k^2 \mathcal{G}_{-\sigma}(-\mathbf{k}, -\omega) \quad \text{(B6)}$$

using the Bogoliubov transformation defined in Eqs. (B4) and (B5). Note that the second term in Eq. (B6) leads to the fermionic hole excitation spectrum with dispersion $E_\mathbf{k}^{(-)}$ [see Eq. (2.25)], even though the excitation energies of the BCS quasiparticles are strictly positive. The residual interaction (2.33) describes the interaction between BCS quasiparticles and their coupling to the collective Bogoliubov-Anderson mode. Explicitly, Eq. (2.33) gives rise to three different types of quasiparticle interactions $\hat{H}_{\text{res}} = \hat{H}_{40} + \hat{H}_{31} + \hat{H}_{22}$ that have been discussed previously, e.g., in nuclear physics [81],

$$\hat{H}_{40} = \frac{g_0}{V} \sum_{\mathbf{k},\mathbf{k}',\mathbf{Q}\neq 0} v_{\mathbf{k}+\mathbf{Q}} v_{\mathbf{k}} u_{\mathbf{k}'} u_{\mathbf{k}'+\mathbf{Q}} \alpha_{\mathbf{k}\uparrow} \alpha_{-\mathbf{k}-\mathbf{Q}\downarrow} \alpha_{-\mathbf{k}'\downarrow} \alpha_{\mathbf{k}'+\mathbf{Q}\uparrow}$$

$$+ \text{H.c.,} \tag{B7}$$

$$\hat{H}_{31} = \frac{g_0}{V} \sum_{\mathbf{k},\mathbf{k}',\mathbf{Q}\neq 0,\sigma} (v_{\mathbf{k}'} v_{\mathbf{k}'+\mathbf{Q}} v_{\mathbf{k}} u_{\mathbf{k}-\mathbf{Q}}$$

$$- u_{\mathbf{k}'} u_{\mathbf{k}'+\mathbf{Q}} u_{\mathbf{k}} v_{\mathbf{k}-\mathbf{Q}}) \alpha^\dagger_{\mathbf{k}\sigma} \alpha_{\mathbf{k}-\mathbf{Q}\sigma} \alpha_{-\mathbf{k}'\downarrow} \alpha_{\mathbf{k}'+\mathbf{Q}\uparrow} + \text{H.c.,}$$

$$\tag{B8}$$

$$\hat{H}_{22} = \frac{g_0}{V} \sum_{\mathbf{k},\mathbf{k}',\mathbf{Q}\neq 0} [(u_{\mathbf{Q}-\mathbf{k}} u_{\mathbf{k}} u_{\mathbf{k}'} u_{\mathbf{Q}-\mathbf{k}'}$$

$$+ v_{\mathbf{Q}-\mathbf{k}} v_{\mathbf{k}} v_{\mathbf{k}'} v_{\mathbf{Q}-\mathbf{k}'}) \alpha^\dagger_{\mathbf{Q}-\mathbf{k}\uparrow} \alpha^\dagger_{\mathbf{k}\downarrow} \alpha_{\mathbf{k}'\downarrow} \alpha_{\mathbf{Q}-\mathbf{k}'\uparrow}$$

$$+ (u_{\mathbf{k}} u_{\mathbf{k}'-\mathbf{Q}} v_{\mathbf{k}'} v_{\mathbf{k}-\mathbf{Q}}$$

$$+ v_{\mathbf{k}} v_{\mathbf{k}'-\mathbf{Q}} u_{\mathbf{k}'} u_{\mathbf{k}-\mathbf{Q}}) \alpha^\dagger_{\mathbf{k}\uparrow} \alpha^\dagger_{-\mathbf{k}'\downarrow} \alpha_{\mathbf{Q}-\mathbf{k}'\downarrow} \alpha_{\mathbf{k}-\mathbf{Q}\uparrow}$$

$$+ u_{\mathbf{k}+\mathbf{Q}} u_{\mathbf{k}'+\mathbf{Q}} v_{\mathbf{k}} v_{\mathbf{k}'} \alpha^\dagger_{\mathbf{k}+\mathbf{Q}\uparrow} \alpha^\dagger_{\mathbf{k}'\uparrow} \alpha_{\mathbf{k}'+\mathbf{Q}\uparrow} \alpha_{\mathbf{k}\uparrow}$$

$$+ v_{\mathbf{k}+\mathbf{Q}} v_{\mathbf{k}'+\mathbf{Q}} u_{\mathbf{k}} u_{\mathbf{k}'} \alpha^\dagger_{\mathbf{k}+\mathbf{Q}\downarrow} \alpha^\dagger_{\mathbf{k}'\downarrow} \alpha_{\mathbf{k}'+\mathbf{Q}\downarrow} \alpha_{\mathbf{k}\downarrow}] \tag{B9}$$

corresponding to four-wave annihilation, quasiparticle decay, and quasiparticle scattering. The only processes that limit the lifetime of a quasiparticle excitation at zero temperature are the decay into three (or more) quasiparticles and the emission of a Bogoliubov-Anderson phonon or a combination thereof. The decay into three quasiparticles via H_{31} has a threshold energy of 3Δ and is forbidden in a rather broad range around the dispersion minimum. As discussed above, the emission of a Bogoliubov-Anderson phonon has a much less restrictive kinematic constraint and thus is the relevant lifetime-limiting process close to the dispersion minimum. In order to estimate this contribution, we need to know how the BCS quasiparticles couple to the collective Bogoliubov-Anderson mode. It is important to notice that the phonons in Hamiltonian (B1) are not independent excitations but are actually bound states of two BCS quasiparticles. Indeed, as shown already by Galitskii [82], the vertex function $\Gamma(\mathbf{q},\omega)$ for the scattering of an up- and a down-BCS quasiparticle with total energy ω and total momentum $\mathbf{q}$ has a pole at $\omega^2 = c_s^2 q^2$ corresponding to the Bogoliubov-Anderson phonon mode. Within a diagrammatic formulation, the leading order self-energy contribution to the BCS quasiparticle Green's function $\mathcal{G}$ corresponding to the emission of a Bogoliubov-Anderson phonon is thus given by the diagram shown in Fig. 7. Explicitly, this gives rise to an imaginary part of the retarded self-energy given by

$$\text{Im}\,\Sigma^R_\sigma(\mathbf{k},\omega) = \int \frac{d^3q\, d^3k'\, d^3k''}{(2\pi)^9} V^{(1,3)}_{\mathbf{k},\mathbf{q},\mathbf{k}'} V^{(3,1)}_{\mathbf{k},\mathbf{q},\mathbf{k}''} Z_{\text{BA}}(q)$$

$$\times \delta(\omega - E_{\mathbf{k}-\mathbf{q}} - c_s|\mathbf{q}|)$$

$$\times \text{Re}\,\mathcal{G}_{-\sigma}(\mathbf{k}',\omega - E_{\mathbf{k}-\mathbf{q}} - E_{\mathbf{q}-\mathbf{k}'})$$
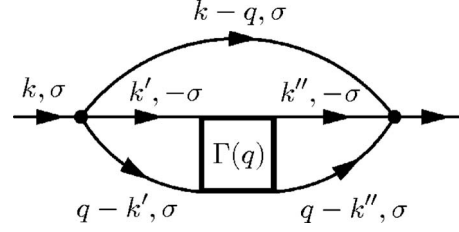

FIG. 7. Dominant contribution to the BCS-quasiparticle self-energy at zero temperature.

$$\times \text{Re}\,\mathcal{G}_{-\sigma}(\mathbf{k}'',\omega - E_{\mathbf{k}-\mathbf{q}} - E_{\mathbf{q}-\mathbf{k}''}) + \cdots, \tag{B10}$$

where $Z_{\text{BA}}(q)$ denotes the quasiparticle weight of the Bogoliubov-Anderson mode and $V^{(1,3)}$ is the bare vertex related to H_{31}. The dots indicate two more terms coming from the imaginary parts of the two BCS quasiparticle Green's functions in Eq. (B10). However, these terms are not important close to the minimum of the dispersion curve, since they give rise to a kinematic constraint related to the decay into three quasiparticles which has a threshold energy of 3Δ.

Assuming that the real part of the self-energy is small, we evaluate the self-energy at $\omega = E_{\mathbf{k}}$ and extract from Eq. (B10) the kinematic constraint (B2). Thus, in the weak-coupling limit, the spectral function exhibits sharp peaks in an exponentially small interval

$$\frac{|k-k_F|}{k_F} < \frac{c_s}{2v_F} \frac{\Delta}{\varepsilon_F} \tag{B11}$$

around the minimum of the dispersion relation. Extrapolated to unitarity, the range where no broadening of the spectral function is expected is $|k-k_\mu| \lesssim 0.1 k_F$. In the BEC regime, where the chemical potential is negative and the minimum of the dispersion relation is at $\mathbf{k}=0$, Eq. (B2) indicates that the spectral function is sharp for momenta $k < mc_s$.

Interestingly, kinematic constraint (B2) that leads to an infinite lifetime of the fermionic excitations around the dispersion minimum is implicitly also present in our Luttinger-Ward theory. Indeed, if Eq. (2.11) is reformulated in terms of mean-field Green's functions, the second term corresponds exactly to the self-energy contribution coming from the virtual emission of a Bogoliubov-Anderson phonon due to the phonon pole of the vertex function Γ. Again, this process causes constraint (B2). Nevertheless, our numerics show a finite lifetime at the dispersion minimum. Apart from the fact that a sharp feature in the spectral function can hardly be resolved numerically, we attribute the finite lifetime to the self-consistent solution of the equations, since the replacement of bare with dressed Green's functions gives rise to diagrams that explicitly violate the Pauli principle.

[1] X. G. Wen, *Quantum Field Theory of Many-Body Systems* (Oxford University Press, New York, 2004).

[2] S. Sachdev, *Quantum Phase Transitions* (Cambridge University Press, Cambridge, England, 1999).

[3] W. Ketterle and M. W. Zwierlein, in *Proceedings of the International School of Physics "Enrico Fermi," Course CLXIV, Varenna, 2006*, edited by M. Inguscio, W. Ketterle, and C. Salomon (IOS Press, Amsterdam, 2008).

[4] I. Bloch, J. Dalibard, and W. Zwerger, Rev. Mod. Phys. **80**, 885 (2008).

[5] S. Giorgini, L. P. Pitaevskii, and S. Stringari, Rev. Mod. Phys. **80**, 1215 (2008).

[6] C. A. Regal, M. Greiner, and D. S. Jin, Phys. Rev. Lett. **92**, 040403 (2004).

[7] M. Bartenstein, A. Altmeyer, S. Riedl, S. Jochim, C. Chin, J. H. Denschlag, and R. Grimm, Phys. Rev. Lett. **92**, 203201 (2004).

[8] J. Kinast, S. L. Hemmer, M. E. Gehm, A. Turlapov, and J. E. Thomas, Phys. Rev. Lett. **92**, 150402 (2004).

[9] M. W. Zwierlein, J. R. Abo-Shaeer, A. Schirotzek, C. H. Schunck, and W. Ketterle, Nature (London) **435**, 1047 (2005).

[10] C. Chin, M. Bartenstein, A. Altmeyer, S. Riedl, S. Jochim, J. Hecker Denschlag, and R. Grimm, Science **305**, 1128 (2004).

[11] J. Kinnunen, M. Rodriguez, and P. Törmä, Science **305**, 1131 (2004).

[12] M. Punk and W. Zwerger, Phys. Rev. Lett. **99**, 170404 (2007).

[13] G. Baym, C. J. Pethick, Z. Yu, and M. W. Zwierlein, Phys. Rev. Lett. **99**, 190407 (2007).

[14] A. Perali, P. Pieri, and G. C. Strinati, Phys. Rev. Lett. **100**, 010402 (2008).

[15] S. Basu and E. J. Mueller, Phys. Rev. Lett. **101**, 060405 (2008).

[16] C. H. Schunck, Y. Shin, A. Schirotzek, M. W. Zwierlein, and W. Ketterle, Science **316**, 867 (2007).

[17] Y. Shin, C. H. Schunck, A. Schirotzek, and W. Ketterle, Phys. Rev. Lett. **99**, 090403 (2007).

[18] Y. Shin, C. H. Schunck, A. Schirotzek, and W. Ketterle, Nature (London) **451**, 689 (2008).

[19] J. T. Stewart, J. P. Gaebler, and D. S. Jin, Nature (London) **454**, 744 (2008).

[20] T. L. Dao, A. Georges, J. Dalibard, C. Salomon, and I. Carusotto, Phys. Rev. Lett. **98**, 240402 (2007).

[21] R. Haussmann, W. Rantner, S. Cerrito, and W. Zwerger, Phys. Rev. A **75**, 023610 (2007).

[22] R. Haussmann and W. Zwerger, Phys. Rev. A **78**, 063602 (2008).

[23] S. Tan, Ann. Phys. **323**, 2971 (2008).

[24] E. Braaten and L. Platter, Phys. Rev. Lett. **100**, 205301 (2008).

[25] D. T. Son and M. Wingate, Ann. Phys. **321**, 197 (2006).

[26] R. Haussmann, *Self-Consistent Quantum-Field Theory and Bosonization for Strongly Correlated Electron Systems*, Lecture Notes in Physics M56 (Springer, Berlin, 1999).

[27] J. M. Luttinger and J. C. Ward, Phys. Rev. **118**, 1417 (1960).

[28] R. Haussmann, Z. Phys. B **91**, 291 (1993).

[29] D. S. Petrov, C. Salomon, and G. V. Shlyapnikov, Phys. Rev. Lett. **93**, 090404 (2004).

[30] D. J. Thouless, Ann. Phys. (N.Y.) **10**, 553 (1960).

[31] E. Burovski, N. Prokof'ev, B. Svistunov, and M. Troyer, Phys. Rev. Lett. **96**, 160402 (2006).

[32] E. Burovski, E. Kozik, N. Prokof'ev, B. Svistunov, and M. Troyer, Phys. Rev. Lett. **101**, 090402 (2008).

[33] A. Bulgac, J. E. Drut, and P. Magierski, Phys. Rev. A **78**, 023625 (2008).

[34] P. Arnold, J. E. Drut, and D. T. Son, Phys. Rev. A **75**, 043605 (2007).

[35] Y. Nishida, Phys. Rev. A **79**, 013627 (2009).

[36] J. Carlson, S.-Y. Chang, V. R. Pandharipande, and K. E. Schmidt, Phys. Rev. Lett. **91**, 050401 (2003); S.-Y. Chang, V. R. Pandharipande, J. Carlson, and K. E. Schmidt, Phys. Rev. A **70**, 043602 (2004).

[37] G. E. Astrakharchik, J. Boronat, J. Casulleras, and S. Giorgini, Phys. Rev. Lett. **93**, 200404 (2004).

[38] H. Hu, X. J. Liu, and P. D. Drummond, Europhys. Lett. **74**, 574 (2006).

[39] R. B. Diener, R. Sensarma, and M. Randeria, Phys. Rev. A **77**, 023626 (2008).

[40] A. W. Fetter and J. D. Walecka, *Quantum Theory of Many-Particle Systems* (McGraw-Hill, New York, 1971).

[41] G. Baym and N. D. Mermin, J. Math. Phys. **2**, 232 (1961).

[42] M. Jarrell and J. E. Gubernatis, Phys. Rep. **269**, 133 (1996).

[43] J. Dukelsky, S. Pittel, and G. Sierra, Rev. Mod. Phys. **76**, 643 (2004).

[44] C. Chin and P. S. Julienne, Phys. Rev. A **71**, 012713 (2005).

[45] W. Schneider, V. B. Shenoy, and M. Randeria, e-print arXiv:0903.3006; note that, in contrast to our discussion of the balanced superfluid, Schneider *et al.* consider the case of an imbalanced *normal* Fermi liquid. The relation (2.37), however, is valid in both cases.

[46] G. B. Partridge, K. E. Strecker, R. I. Kamar, M. W. Jack, and R. G. Hulet, Phys. Rev. Lett. **95**, 020404 (2005).

[47] F. Werner, L. Tarruell, and Y. Castin, Eur. Phys. J. B **68**, 401 (2009).

[48] S. Zhang and A. J. Leggett, Phys. Rev. A **77**, 033614 (2008).

[49] S. Zhang and A. J. Leggett, Phys. Rev. A **79**, 023601 (2009).

[50] A. A. Abrikosov, L. P. Gorkov, and I. E. Dzyaloshinskii, *Methods of Quantum Field Theory in Statistical Physics* (Dover, New York, 1963); see, e.g., Chap. I.5.

[51] S. Tan, Ann. Phys. **323**, 2952 (2008).

[52] Z. Yu, G. M. Bruun, and G. Baym, Phys. Rev. A **80**, 023615 (2009).

[53] M. Tinkham, *Introduction to Superconductivity* (McGraw-Hill, New York, 1996).

[54] J. R. Engelbrecht, M. Randeria, and C. A. R. Sa de Melo, Phys. Rev. B **55**, 15153 (1997).

[55] Z. Nussinov and S. Nussinov, Phys. Rev. A **74**, 053622 (2006).

[56] Y. Nishida and D. T. Son, Phys. Rev. Lett. **97**, 050403 (2006).

[57] G. Rupak and T. Schäfer, Nucl. Phys. A **816**, 52 (2009).

[58] It is easy to see that $c_2=0$ in the BEC limit implying a vanishing pair size. This is a consequence of the relation $n_s(q) \equiv n$ for arbitrary wave vectors q that holds for a weakly interacting BEC described within Bogoliubov theory. The latter is appropriate in the molecular limit of the BCS-BEC crossover with dimer-dimer scattering length $a_{dd}=0.6a$.

[59] R. Sensarma (private communication).

[60] M. Brack and R. K. Bhaduri, *Semiclassical Physics* (Addison-Wesley, Reading, MA, 1997).

[61] Note that the Weizsäcker inhomogeneity correction has precisely the form of the quantum pressure contribution in the Gross-Pitaevskii theory of a Bose superfluid, which describes

the ground state of the BCS-BEC crossover in the molecular limit. Accounting for the factors 2 in the associated Bose mass or density, the corresponding value of b in this limit consistent with Eq. (3.6) is $b = 1/16 = 0.0625$.

[62] Y. Nishida and D. T. Son, Phys. Rev. A **75**, 063617 (2007).

[63] D. T. Son and M. A. Stephanov, Phys. Rev. A **74**, 013614 (2006).

[64] J. Carlson and S. Reddy, Phys. Rev. Lett. **95**, 060401 (2005)

[65] A. Schirotzek, Y. I. Shin, C. H. Schunck, and W. Ketterle, Phys. Rev. Lett. **101**, 140403 (2008).

[66] C. L. Kane, P. A. Lee, and N. Read, Phys. Rev. B **39**, 6880 (1989).

[67] P. Magierski, G. Wlazlowski, A. Bulgac, and J. E. Drut, Phys. Rev. Lett. (in print).

[68] For the case of quasiparticle decay due to single phonon emission, there is actually a shell of finite thickness in momentum space where the width vanishes identically at $T=0$.

[69] M. R. Norman, M. Randeria, H. Ding, and J. C. Campuzano, Phys. Rev. B **57**, R11093 (1998).

[70] Q. Chen and K. Levin, Phys. Rev. Lett. **102**, 190402 (2009).

[71] T.-L. Dao, I. Carusotto, and A. Georges, Phys. Rev. A **80**, 023627 (2009).

[72] Q. Chen, K. Levin, and I. Kosztin, Phys. Rev. B **63**, 184519 (2001).

[73] A. Perali, P. Pieri, G. C. Strinati, and C. Castellani, Phys. Rev. B **66**, 024510 (2002).

[74] P. Pieri, L. Pisani, and G. C. Strinati, Phys. Rev. B **70**, 094508 (2004).

[75] S. Moukouri, S. Allen, F. Lemay, B. Kyung, D. Poulin, Y. M. Vilk, and A.-M. S. Tremblay, Phys. Rev. B **61**, 7887 (2000).

[76] D. Sivia and J. Skilling, *Data Analysis: A Bayesian Tutorial* (Oxford University Press, Oxford, 2006).

[77] R. K. Bryan, Eur. Biophys. J. **18**, 165 (1990).

[78] N. Lerch, L. Bartosch, and P. Kopietz, Phys. Rev. Lett. **100**, 050403 (2008).

[79] J. Carlson and S. Reddy, Phys. Rev. Lett. **100**, 150403 (2008).

[80] B. Mühlschlegel, J. Math. Phys. **3**, 522 (1962).

[81] P. Ring and P. Schuck, *The Nuclear Many-Body Problem* (Springer, Berlin, 2000).

[82] V. M. Galitskii, Sov. Phys. JETP **7**, 698 (1958).